Statistical Methods

The difference in the serum *M/N* ratio between the MNA and non-MNA groups was assessed using the Mann-Whitney *U* test. $P < .05$ was judged as significant.

RESULTS

Serum M/N Ratio As a Predictor of MYCN Status of Tumor

Serum *M/N* ratios could be determined in approximately 4 hours by real-time quantitative PCR. Figure 1 shows the distribution of the serum *M/N* ratio in the MNA and non-MNA groups at the time of diagnosis. The serum *M/N* ratio in the MNA group (n = 17; median, 199.32; range, 17.1 to 901.6; 99% CI, 107.0 to 528.7) was significantly ($P < .001$) higher than the ratio in the non-MNA group (n = 70; median, 0.87; range, 0.25 to 4.6; 99% CI, 0.82 to 1.26). In fact, there was no overlap between the two groups in the limited number of patients examined in this study. As a cutoff for the serum *M/N* ratio to distinguish between MNA and non-MNA patients, we empirically chose a value of 10, which was in the middle of the two ranges. With this value, the sensitivity and specificity of the serum *M/N* ratio as a diagnostic test to distinguish patients with MNA from those without MNA were both 100% for our limited number of patients. That is, the serum *M/N* ratio was in complete agreement with the Southern blotting results. The positive and negative predictive values were 100%. The serum *M/N* ratios were also consistent with results obtained by FISH for 45 of the patients (FISH analyses were performed in 12 of the 17 MNA patients and in 33 of the 70 nonamplified patients). Three of the patients who had one to four extra copies of the *MYCN* gene relative to chromosome 2 centromere number, as determined by FISH, also had slightly elevated serum *M/N* ratios (2.5, 3.3, and 4.6).

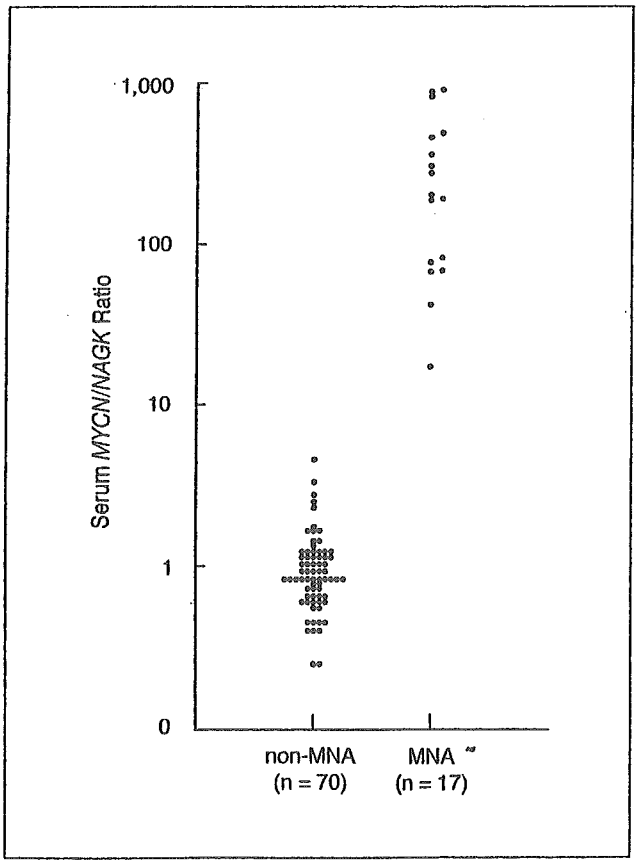

Fig 1. A scatter plot of serum *MYCN/NAGK* ratio in patients with *MYCN*-amplified (MNA) and nonamplified (non-MNA) neuroblastoma. The serum *MYCN/NAGK* ratio was significantly ($P < .001$) higher in the MNA group (median, 199.32; range, 17.1 to 901.6; 99% CI, 107.0 to 528.7) than in the non-MNA group (median, 0.87; range, 0.25 to 4.6; 99% CI, 0.82 to 1.26; Mann-Whitney *U* test).

Change in Serum M/N Ratio Levels During Follow-Up

To evaluate whether an increase in the serum *M/N* ratio can be used as an indicator of relapse, we measured serum *M/N* ratios at several points in the clinical courses of six patients with MNA (Fig 2). In three patients who were in complete remission (patients 1, 2, and 3), the serum *M/N* ratios decreased to the normal range and were consistently low. In contrast, in one patient who failed to achieve remission (patient 4), the serum *M/N* ratio did not decrease to the normal range and remained at a high level until his death. In the other patients who experienced recurrence after remission (patients 5 and 6), the serum *M/N* ratio first decreased to the normal range and then increased beyond the cutoff value by the time of diagnosis.

Effect of WBC Contamination on Serum M/N Ratio

We found that a high serum *M/N* ratio could be masked by the presence of WBC. The *M/N* ratio of serum from an *MYCN*-amplified patient decreased with increasing WBC contamination (Fig 3). When 200 μL of serum was contaminated with 1×10^5 of WBC, corresponding to approximately one fortieth of the WBC concentration in normal whole blood, the serum *M/N* ratio decreased below the cutoff level.

DISCUSSION

Serum markers, such as ferritin,[19] lactic dehydrogenase,[20] and neuron-specific enolase,[21] have been proposed as prognostic markers of NB, although they have shown little prognostic value. Recently, elevated levels of plasma midkine have been reported to correlate with a poor prognosis. However, the significance of this finding is controversial because plasma midkine levels are highest in stage 4S patients.[22] Therefore, a noninvasive assay of tumor-related

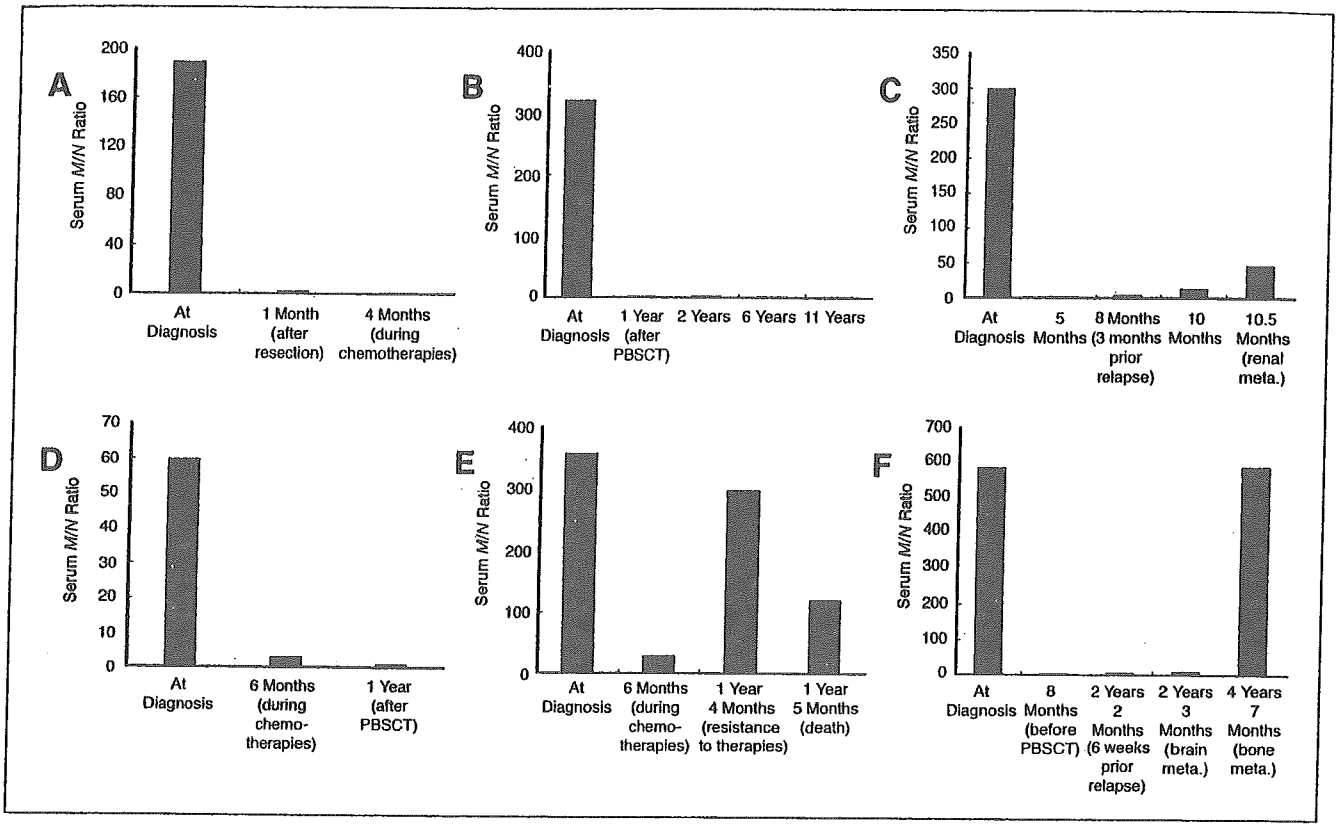

Fig 2. Changes in serum *MYCN/NAGK* (*M/N*) ratio levels of six patients with *MYCN* amplification during follow-up. PBSCT, peripheral-blood stem-cell transfusion; meta., metastasis. (A) Patient 1; (B) patient 3; (C) patient 5; (D) patient 2; (E) patient 4; (F) patient 6.

genetic aberrations using serum DNA is desirable for the assessment of prognosis and therapy stratification at the time of diagnosis. Among the tumor-related genetic aberrations detected in NB, MNA was of greatest interest to us because of its significant prognostic value.

By using DNA-based real-time quantitative PCR with a single-copy reference gene, we have demonstrated that the *M/N* ratio in serum DNA is a valuable diagnostic tool to discriminate MNA patients from non-MNA patients. The serum *M/N* ratio in the MNA group was significantly higher than the ratio in the non-MNA group, without an overlap. The highest sensitivity (100%), highest specificity (100%), highest positive predictive value (100%), and highest negative predictive value (100%) were obtained with a serum *M/N* ratio cutoff value of 10.0. Furthermore, we found an elevated level of the serum *M/N* ratio in a stage 1 patient and a stage 2B patient with MNA (188.7 and 901.6, respectively), even though the tumor was localized in these patients. This suggests that tumors could release a significant amount of genomic DNA into the systemic circulation even at an early stage. Furthermore, Sozzi et al[23] reported that the concentration of plasma DNA in 84 lung cancer patients was higher than the concentration in 43 controls, regardless of the tumor stage, and suggested that circulating DNA in peripheral blood was an early event in lung carcinogenesis.

Another clinical benefit of the serum *M/N* assay is that it could be used as a marker to monitor therapeutic efficacy and recurrence after therapies. The serum *M/N* ratio decreased to the normal range in the patients in remission but remained at a high level in the patient who failed to achieve remission. Furthermore, in two patients with recurrence after remission, the serum *M/N* ratio initially decreased to the normal range but then increased beyond the cutoff value by the time of diagnosis. The serum *M/N* ratio did not increase to the initial level as long as the metastasis was localized in the brain, but it did increase to the initial level when the patient later developed a bone metastasis (patient 6). This is noteworthy because it suggests that a brain metastasis releases genomic DNA into the systemic circulation less easily than extracranial tumors. If this is confirmed by examination of additional patients, then it is possible that tumors localized in brain could be overlooked with diagnostic assays based on serum DNA.

A possible pitfall of our serum *M/N* assay is that a high serum *M/N* ratio could be reduced by WBC contamination (Fig 3). This could be a result of dilution of tumor DNA with the WBC DNA, which would be expected to have an *M/N* ratio of 1. Therefore, the importance of removing WBCs from serum should be addressed in diagnostic assays

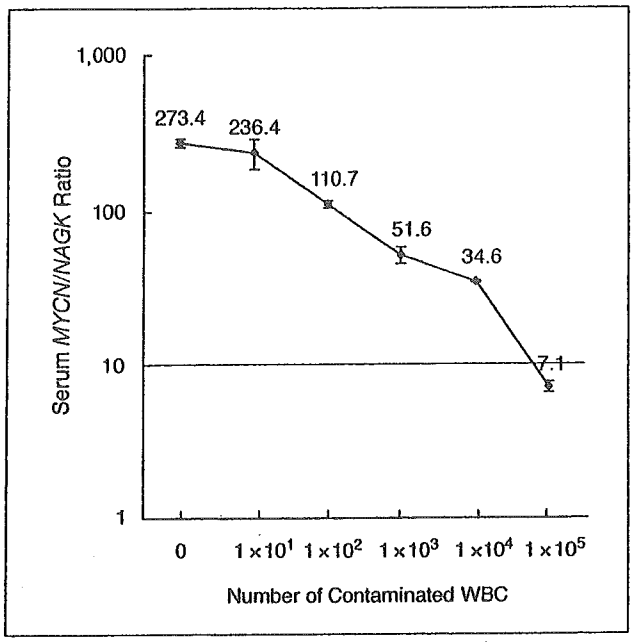

Fig 3. Influence of WBC contamination in serum samples on the serum *MYCN/NAGK* ratio. Data are presented as the mean ± standard deviation of duplicate measurements. The transverse line represents a *MYCN/NAGK* ratio cutoff value of 10.0.

that use serum DNA. For the same reason, a predominance of any nontumor DNA in serum may lower an elevated *M/N* ratio of an *MYCN*-amplified patient. However, this assay can be accurate on the premise that, in cancer patients, serum DNA predominantly consists of tumor-released DNA.[7] In addition, the use of serum DNA as a diagnostic tool in lung cancer patients has resulted in a diversity of findings, suggesting that these differences likely reflect variations in the manner in which the blood specimens were collected and handled and variations in the methods by which the assay were conducted.[24] Therefore, it is necessary to standardize the serum collection procedure to ensure that different laboratories obtain the same result with a given blood sample. An additional high-speed centrifugation step (16,000 × *g* for 5 minutes) was found to eliminate cellular contamination even after thawing of stored samples.[25] By using the appropriate centrifugation methods, we believe that WBC-free serum can be reliably achieved.

Although a large set of patients needs to be studied to verify the accuracy of this assay and to set an appropriate cutoff, our results are promising and need to be further tested. The advantages of this method are that it takes only 4 hours and much less effort than FISH and Southern blotting, which should make this assay an alternative to these other methods for determining *MYCN* status. A third advantage is that the serum *M/N* ratio seems to be a promising indicator of therapeutic efficacy and relapse in the follow-up of patients with MNA, although more patients need to be examined to confirm its reliability.

Acknowledgment

We thank two anonymous reviewers for helpful comments.

Authors' Disclosures of Potential Conflicts of Interest

The authors indicated no potential conflicts of interest.

REFERENCES

1. Brodeur GM, Seeger RC, Schwab M, et al: Amplification of N-myc in untreated human neuroblastomas correlates with advanced disease stage. Science 224:1121-1124, 1984
2. Seeger RC, Brodeur GM, Sather H, et al: Association of multiple copies of the N-myc oncogene with rapid progression of neuroblastomas. N Engl J Med 313:1111-1116, 1985
3. Brodeur GM, Maris JM, Yamashiro DJ, et al: Biology and genetics of human neuroblastomas. J Pediatr Hematol Oncol 19:93-101, 1997
4. Brodeur GM, Pritchard J, Berthold F, et al: Revisions of the international criteria for neuroblastoma diagnosis, staging and response to treatment. J Clin Oncol 11:1466-1477, 1993
5. Castleberry RP, Prichard J, Ambros P, et al: The International Neuroblastoma Risk Groups (INRG): A preliminary report. Eur J Cancer 33: 2113-2116, 1997
6. Shimada H, Ambros IM, Dehner LP, et al: The International Neuroblastoma Pathology Classification System (the Shimada system). Cancer 86:364-372, 1999
7. Shapiro B, Chakrabarty M, Cohn EM, et al: Determination of circulating DNA levels in patients with benign or malignant gastrointestinal disease. Cancer 51:2116-2120, 1983
8. Sozzi G, Conte D, Leon M, et al: Quantification of free circulating DNA as a diagnostic marker in lung cancer. J Clin Oncol 21:3902-3908, 2003
9. Sozzi G, Musso K, Ratcliffe C, et al: Detection of microsatellite alterations in plasma DNA of non-small cell lung cancer patients: A prospect for early diagnosis. Clin Cancer Res 5:2689-2692, 1999
10. Chen X, Bonnefoi H, Diebold-Berger S, et al: Detecting tumor-related alterations in plasma or serum DNA of patients diagnosed with breast cancer. Clin Cancer Res 5:2297-2303, 1999
11. Silva JM, Dominguez G, Garcia JM, et al: Presence of tumor DNA in plasma of breast cancer patients: Clinicopathological correlations. Cancer Res 59:3251-3256, 1999
12. Combaret V, Audoynaud C, Iacono I, et al: Circulating *MYCN* DNA as a tumor-specific marker in neuroblastoma patients. Cancer Res 62:3646-3648, 2002
13. Akiyama K, Kanda N, Yamada M, et al: Megabase-scale analysis of the origin of N-myc amplicons in human neuroblastoma. Nucleic Acids Res 22:187-193, 1994
14. Gotoh T, Sugihara H, Matsumura T, et al: Human neuroblastoma demonstrating clonal evolution in vivo. Genes Chromosomes Cancer 22:42-49, 1998
15. Spitz R, Hero B, Skowron M, et al: *MYCN*-status in neuroblastoma: Characteristics of tumours showing amplification, gain, and non-amplification. Eur J Cancer 40:2753-2759, 2004
16. Gelmini S, Orlando C, Sestini R, et al: Quantitative polymerase chain reaction-based homogeneous assay with fluorogenic probes to measure c-erbB-2 oncogene amplification. Clin Chem 43:752-758, 1997
17. Claudia CR, Maria LB, Gian PT, et al: Real-time quantitative PCR for the measurement of *MYCN* amplification in human neuroblastoma with the TaqMan detection system. Clin Chem 45:1918-1924, 1999
18. Chiang PW, Beer DG, Wei WL, et al: Detection of erbB-2 amplifications in tumors and sera from esophageal carcinoma patients. Clin Cancer Res 5:1381-1386, 1999
19. Hann HWL, Evans AE, Siegel SE, et al: Prognostic importance of serum ferritin in patients with stage III and IV neuroblastoma: The

Children's Cancer Study Group experience. Cancer Res 45:2843-2848, 1985

20. Quinn JJ, Altman AJ, Frantz CN, et al: Serum lactic dehydrogenase, an indicator of tumor activity in neuroblastoma. J Pediatr 97:89-91, 1980

21. Massaron S, Seregni E, Luksch R, et al: Neuron-specific enolase evaluation in patients neuroblastoma. Tumour Biol 19:261-268, 1998

22. Ikematsu S, Nakagawara A, Nakamura Y, et al: Correlation of elevated level of blood midkine with poor prognostic factors of human neuroblastomas. Br J Cancer 88:1522-1526, 2003

23. Sozzi G, Conte D, Mariani L, et al: Analysis of circulating tumor DNA in plasma at diagnosis and during follow-up of lung cancer patients. Cancer Res 61:4675-4678, 2001

24. Bunn PA: Early detection of lung cancer using serum RNA or DNA markers: Ready for "prime time" or for validation? J Clin Oncol 21:3891-3893, 2003

25. Swinkels DW, Wiegerinck E, Steegers EAP, et al: Effect of blood-processing protocols on cell-free DNA quantification in plasma. Clin Chem 49:525-526, 2003

American Journal of Pathology, Vol. 167, No. 1, July 2005

Tumorigenesis and Neoplastic Progression

Biological Role of Anaplastic Lymphoma Kinase in Neuroblastoma

Yuko Osajima-Hakomori,*¶‖ Izumi Miyake,*† Miki Ohira,‡ Akira Nakagawara,‡ Atsuko Nakagawa,§ and Ryuichi Sakai*

From the Growth Factor Division, National Cancer Center Research Institute, Chuo-ku, Tokyo; St. Marianna University School of Medicine,¶ Kawasaki-shi, Kanagawa; Tokyo Metropolitan Geriatric Hospital,‖ Itabashi-ku, Tokyo; the Department of Pediatrics,† Kitasato University School of Medicine, Sagamihara-shi, Kanagawa; the Division of Biochemistry,‡ Chiba Cancer Center Research Institute, Cyuo-ku, Chiba; and the Department of Pathology,§ Aichi Medical University, Aichi-gun, Aichi, Japan*

Anaplastic lymphoma kinase (ALK) is a tyrosine kinase receptor originally identified as part of the chimeric nucleophosmin-ALK protein in the t(2;5) chromosomal rearrangement associated with anaplastic large cell lymphoma. We recently demonstrated that the ALK kinase is constitutively activated by gene amplification at the ALK locus in several neuroblastoma cell lines. Forming a stable complex with hyperphosphorylated ShcC, activated ALK modifies the responsiveness of the mitogen-activated protein kinase pathway to growth factors. In the present study, the biological role of activated ALK was examined by suppressing the expression of ALK kinase in neuroblastoma cell lines using an RNA interference technique. The suppression of activated ALK in neuroblastoma cells by RNA interference significantly reduced the phosphorylation of ShcC, mitogen-activated protein kinases, and Akt, inducing rapid apoptosis in the cells. By immunohistochemical analysis, the cytoplasmic expression of ALK was detected in most of the samples of neuroblastoma tissues regardless of the stage of the tumor, whereas significant amplification of ALK was observed in only 1 of 85 cases of human neuroblastoma samples. These data demonstrate the limited frequency of ALK activation in the real progression of neuroblastoma. *(Am J Pathol 2005, 167:213–222)*

Receptor tyrosine kinases (RTKs) play an important role in regulating diverse cellular processes, such as proliferation, differentiation, survival, motility, and malignant transformation. The activation of RTKs typically requires ligand-induced receptor oligomerization, which results in tyrosine autophosphorylation of the receptors at tyrosine residues.[1–3] By recruiting specific sets of signal transducer molecules in a phosphorylation-dependent manner, each RTK is capable of inducing individual, specific cellular responses.[4] On the other hand, activation of RTKs by either mutations or overexpression is frequently found in various human malignancies.[3,5]

Anaplastic lymphoma kinase (ALK) is a 200-kd tyrosine kinase encoded by the *ALK* gene on chromosome 2p23. ALK was first identified as part of an oncogenic fusion tyrosine kinase, nucleophosmin-ALK, which is associated with anaplastic large cell lymphoma.[6,7] It was also found as a form of fusion protein with a clathrin heavy chain (CTCL) in myofibroblastic tumors.[8] Full-length ALK has the typical structure of an RTK, with a large extracellular domain, a lipophilic transmembrane segment, and a cytoplasmic tyrosine kinase domain.[9,10] ALK is highly homologous to leukocyte tyrosine kinase (LTK) and is further classified into the insulin receptor superfamily. The *LTK* gene is mainly expressed in pre-B lymphocytes and neuronal tissues,[11–13] whereas expression of the normal *ALK* gene in hematopoietic tissues has not been detected. Instead, it is dominantly expressed in the neural system.[14,15] In the developing brains of mice, specific expression of *ALK* was seen in the thalamus, mid-brain, olfactory bulb, and selected cranial regions, as well as the dorsal root, the ganglia of mice,[9,10,16] suggesting a specific role in the development of the embryonic nervous system. Currently, however, the function of ALK in adult normal tissue or carcinogenesis remains an open question. Several studies have recently indicated pleiotrophin or midkine as possible ligands for ALK.[17,18] Although they appeared to induce the functional activa-

Supported by the Program for the Promotion of Fundamental Studies in Health Science of the Organization for Pharmaceutical Safety and Research of Japan. Y.O-H. is the recipient of a Research Resident Fellowship from the Foundation for Promotion of Cancer Research, Japan.

Accepted for publication March 23, 2005.

Address reprint requests to Ryuichi Sakai, M.D., Growth Factor Division, National Cancer Center Research Institute, 5-1-1 Tsukiji, Chuo-ku, Tokyo 104-0045, Japan. E-mail: rsakai@gan2.res.ncc.go.jp.

tion of ALK, it is still unclear whether these molecules are the physiological ligands of ALK.

Neuroblastoma is one of the most common pediatric tumors derived from the sympathoadrenal linage of the neural crest. Tumors found in patients under the age of 1 year are usually favorable and often show spontaneous differentiation and regression.[19] Amplification of the N-*myc* gene occurs in approximately 25% of neuroblastomas and correlates with the aggressiveness of the disease. In addition to N-*myc* gene amplification, the expression of various genes has significant correlation with the stage of and prognosis for neuroblastoma. A high level of TrkA expression is predictive of a favorable outcome,[20] whereas TrkB is highly expressed in immature neuroblastomas with N-*myc* amplification.[21] High expression of caspase-1, -3, and -8 is correlated with favorable neuroblastomas.[22,23] On the other hand, survivin, which suppresses caspase and promotes the cell survival signal, is significantly expressed,[24] and telomerase is activated[25] in unfavorable tumors. There may be a critical difference in the expression of other molecules, including RTKs, in neuroblastoma. A recent paper showed that full-length ALK is detected in almost one-half of the cell lines derived from neuroblastomas and neuroectodermal tumors.[26] We have recently shown using mass-spectrometry analysis that ALK is a major phosphoprotein associated with hyperphosphorylated ShcC in several neuroblastoma cell lines.[27] In these cells, ALK was markedly activated, and it induced the constitutive phosphorylation of ShcC and mitogen-activated protein kinase (MAPK), regardless of stimulation by epidermal growth factor (EGF) or nerve growth factor.[27] These findings strongly suggest that constitutively activated ALK kinase plays a physiological role in the development of neuroblastoma.

In this study, we investigated the biological function of the constitutively activated ALK kinase in neuroblastoma. The RNA interference (RNAi) technique using specific sets of small interfering RNA (siRNA) was induced to inhibit the *ALK* gene expression in human neuroblastoma cells with or without gene amplification of *ALK*. The effects of disrupted ALK expression on cell survival or downstream signaling, such as MAPKs or Akt pathways, are examined to understand the biological meaning of ALK amplification in neuroblastoma cells. We also performed Southern blot analysis of primary neuroblastoma tumors from 85 patients to check whether the *ALK* gene amplification was actually present in neuroblastoma tissues. Furthermore, we sought the *ALK* gene expression in human neuroblastoma tissues using immunohistochemical analysis.

Materials and Methods

Cell Culture

Cell lines of human neuroblastoma were maintained in RPMI 1640 supplemented with 10% fetal calf serum (Sigma, St. Louis, MO), penicillin, and streptomycin at 37°C in a humidified 5% CO_2 incubator.

Reverse Transcription-Polymerase Chain Reaction (RT-PCR) Analysis

Total RNA was extracted with ISOGEN (Nippongene Japan, Toyama, Japan) from NB-39-nu and SK-N-MC cells. The PCR primer pair 5′-AGGTTCTGGCTGCAGATGGT-3′ and 5′-ACATTGTTCTCTCGAGTGCAGAC-3′ corresponding to the cytoplasmic portion of human ALK was prepared. As much as 0.25 μg of total RNA was reverse transcribed and amplified with the SuperScript One-step RT-PCR with the Platinum *Taq* kit (Invitrogen Life Technologies, Carlsbad, CA) in a total volume of 50l including 2× reaction mix, 0.2 μmol/L of each primer, and 1 μl of RT/Platinum *Taq* Mix. Amplification conditions consisted of cDNA synthesis and predenaturation at 50°C for 30 minutes and 94°C for 2 minutes followed by 25 cycles at 94°C for 15 seconds, 58°C for 30 seconds, and 72°C for 45 seconds. A final amplification for 7 minutes at 72°C finished the PCR. The product was separated with 1.2% agarose gel electrophoresis and analyzed using the Quality One System (Bio-Rad, Hercules, CA).

Immunochemical Analysis of Proteins

Immunoprecipitation and immunoblotting were performed as described previously.[27] The polyclonal antibodies against the CH1 domains of ShcC (amino acids 306–371) and the anti-ALK antibody (αALK) that was against the cytoplasmic portion (amino acid 1379–1524) of human ALK were prepared as described previously.[27,28] An anti-phosphotyrosine antibody (4G10) was obtained from UBI. Anti-p44/42 MAPKs, anti-phospho-p44/42 MAPKs, anti-Akt, and anti-phospho-Akt antibodies were purchased from Cell Signaling (Beverly, MA). Anti-EGF receptor (EGFR), anti-Ret, and anti-TrkA antibodies were purchased from Santa Cruz Biotechnology (Santa Cruz, CA). *In vitro* kinase assay for ALK was performed as previously described.[27] Anti-ALK immunoprecipitates were incubated with or without Poly-Glu/Tyr as an exogenous substrate.

Immunocytostaining

For ALK/TOTO-3, immunostaining using anti-ALK antibody was performed at first, and then nuclei were stained using TOTO-3. The cells seeded on the 24-well plates were washed with phosphate-buffered saline (PBS) three times and fixed with 4% paraformaldehyde (methanol free) for 5 minutes at room temperature. The cells were rinsed with PBS twice and then permeabilized with 0.2% Triton X-100 solution in PBS for 10 minutes at room temperature. The cells were blocked with 5% goat serum and 3% bovine serum albumin–Tris-buffered saline for 30 minutes at room temperature. The blocking solution was drained off, and the cells were incubated with a 1:1000 dilution of αALK for 1 hour at room temperature. The cells were rinsed with PBS three times and incubated with a 1:2000 dilution of Alexa fluor (Molecular Probes, Eugene, OR) and 1: 100 dilution of TOTO-3 (Molecular Probes) for

Table 1. Patient Characteristics of Neuroblastoma Tissues with *ALK* Gene Gain or Amplification

Case	Age*	Primary tumor		Copy nos. of *ALK*‡	Amplification of N-*myc* (*n*)
		Location	Clinical stage†		
1	3y5m	Adrenal gland	IV	2.0 ± 0.2	+ (35)
2	5y0m	Peritoneum	IV	1.8 ± 0.1	+ (>150)
3	2y7m	Abdomen	IV	2.1 ± 0.8	+ (150)
4	8m	Adrenal gland	I	3.0 ± 1.0	–
5	4y9m	Abdomen	IV	2.0 ± 0.2	–
6	3y9m	Adrenal gland	III	2.7 ± 0.2	+ (>150)
7	1y4m	Adrenal gland	IV	2.8 ± 1.0	+ (150)
8	1y7m	Adrenal gland	IV	9.5 ± 2.2	+ (>100)

*Age of onset: year (y), month (m).
†The staging criterion was based on the International Neuroblastoma Staging System.
‡The averages of the calculated copy numbers from three independent blottings are shown.

30 minutes at room temperature. The cells were washed three times with PBS and mounted in glycerol-based 2.5% 1,4-diazabicyclo[2,2,2] octan. Confocal laser scanning analysis was carried out. For ALK/TUNEL, we first carried out TUNEL and then proceeded to standard immunocytochemistry using anti-ALK antibody. TUNEL was performed using the DeadEnd Fluorometric TUNEL System (Promega, Madison, WI) with the following modifications. The NB-39-nu cells seeded on the 24-well plates that were treated with siRNAs were washed with PBS twice and fixed with 4% paraformaldehyde (methanol free) for 25 minutes at 4°C. The cells were rinsed with PBS twice and then permeabilized with 0.2% Triton X-100 solution in PBS for 5 minutes at room temperature. The cells were washed with PBS twice and covered with an equilibration buffer (from the kit) for 10 minutes at room temperature. The equilibration buffer was drained off, and a reaction buffer containing the equilibration buffer, nucleotide mix, and terminal deoxynucleotidyl transferase enzyme was added to the cells and incubated at 37°C for 1 hour, avoiding exposure to light. The cells were incubated for 15 minutes at room temperature with 2× standard saline citrate to stop the reaction. The cells were washed with PBS three times and then stained for ALK using immunofluorescence as follows. The cells were blocked with 2% bovine serum albumin (Boehringer Mannheim, Germany) for 30 minutes at room temperature. The blocking solution was drained off, and the cells were incubated with a 1:1000 dilution of αALK for 1 hour at room temperature. The cells were rinsed with PBS three times and incubated with a 1:40 dilution of rhodamine-conjugated goat anti-rabbit secondary antibody (Santa Cruz Biotechnology) for 30 minutes at room temperature. The cells were washed three times with PBS and then mounted and observed in the same manner as that for ALK/TOTO-3.

DNA Extraction and Southern Blotting

Genomic DNAs derived from neuroblastoma cell lines were obtained from cultured cells as described using the procedure of Perucho et al.[29] Samples of 85 neuroblastoma tissues were collected at the Chiba Cancer Center and stored as forms of genomic DNA. The characteristics of some of these patients are shown in Table 1. The stage criterion was based on the International Neuroblastoma Staging System.[30] Samples of 5 μg of DNA digested by *Eco*RI were electrophoresed in 0.8% agarose gel and blotted onto nitrocellulose filters (Hybond-N+; Amersham, Piscataway, NJ). The probes for detecting the *ALK* gene, N-*myc* gene, and *ShcC* gene were used in our previous study.[27] The intensities of these signals were measured using a Molecular Imager FxPro (Bio-Rad). This study was approved by the ethical judging committee of the National Cancer Center and the Chiba Cancer Center of Japan.

RNA Interference Technique

Twenty-one-nucleotide double-stranded RNAs were synthesized and purified using Dharmacon Research (Lafayette, CO). To suppress the expression of ALK protein, two different pairs of ALK siRNAs, ALK-siRNA1 and ALK-siRNA2, were obtained. The sequences were 5′-GAGUCUGGCAGUUGACUUCdTdT-3′ for ALK-siRNA1 and 5′-GCUCCGGCGUGCCAAGCAGdTdT-3′ for ALK-siRNA2, corresponding to coding region 153 to 171 and 399 to 417 relative to the first nucleotide of the start codon, respectively. Entire sequences were derived from the sequence of human *ALK* mRNA (accession no. HSU62540). An siRNA, targeting a sequence in the firefly (*Photinus pyralis*) luciferase mRNA, was used as a negative control (Dharmacon) (luc-siRNA). We also used a scramble siRNA, Scramble Duplex II (Dharmacon) (s-siRNA) as a mismatch siRNA control in addition to luc-siRNA.

NB-39-nu cells were trypsinized, diluted with growth medium containing 10% fetal calf serum, and transferred to 12-well plates at 6×10^4 cells per well for 24 hours before transfection. The transfection of siRNA was carried out using jetSI (Poly plus transfection). A total of 100 μl of serum-free growth medium and 4 μl of jetSI per well were preincubated for 5 to 10 minutes at room temperature. While the incubation was being performed, 100 μl of serum-free growth medium was mixed with 5 μl of 20 μmol/L siRNA duplex (100 pmol). Total siRNA amounts of 50, 100, and 200 pmol were checked in preliminary experiments to find out 100 pmol is the minimal and optimal amount in this scale of RNAi. The 100 μl of jetSI serum-free medium solution was added to the 100 μl of siRNA

duplex solution, gently mixed, and incubated for 30 minutes at room temperature. The growth medium on the cells was removed, and 800 μl of serum-free medium was added to each well. A total of 200 μl of the entire mixture was overlaid onto the cells, and cells were incubated for 4 hours at 37°C in a 5% CO_2 incubator. After incubation, 1 ml of medium containing 4% fetal calf serum was added without removing the transfection mixture (final concentration 2%). The cells were assayed 84 hours after transfection. SK-N-MC cells were seeded in 12-well plates at a concentration of 1.3×10^5 cells per well. These were treated with siRNAs in the same way as NB-39-nu and assayed 48 hours after transfection. In the 24-well plate, the cells were seeded at the same concentration as the 12-well plate, and siRNAs and all other reagents were used at half volume. After transfection, the cells were examined under a light microscope every day.

Double Staining for ALK and TUNEL

For double staining, we first carried out TUNEL and then proceeded to standard immunocytochemistry using anti-ALK antibody. TUNEL was performed using the DeadEnd Fluorometric TUNEL System (Promega) with the following modifications. The NB-39-nu cells seeded on the 24-well plates that were treated with siRNAs were washed with PBS twice and fixed with 4% paraformaldehyde (methanol free) for 25 minutes at 4°C. The cells were rinsed with PBS twice and then permeabilized with 0.2% Triton X-100 solution in PBS for 5 minutes at room temperature. The cells were washed with PBS twice and covered with an equilibration buffer (from the kit) for 10 minutes at room temperature. The equilibration buffer was drained off, and a reaction buffer containing the equilibration buffer, nucleotide mix, and terminal deoxynucleotidyl transferase enzyme was added to the cells and incubated at 37°C for 1 hour, avoiding exposure to light. The cells were incubated for 15 minutes at room temperature with 2× standard saline citrate to stop the reaction. The cells were washed with PBS three times and then stained for ALK using immunofluorescence as follows. The cells were blocked with 2% bovine serum albumin (Boehringer Mannheim) for 30 minutes at room temperature. The blocking solution was drained off, and the cells were incubated with a 1:1000 dilution of αALK for 1 hour at room temperature. The cells were rinsed with PBS three times and incubated with a 1:40 dilution of rhodamine-conjugated goat anti-rabbit secondary antibody (Santa Cruz Biotechnology) for 30 minutes at room temperature. The cells were washed three times with PBS and mounted in glycerol-based 2.5% 1,4-diazabicyclo[2,2,2] octan. Confocal laser scanning analysis was carried out.

DNA Fragmentation Assay

To detect apoptotic DNA cleavage, DNA fragmentation assay was performed using an Apoptotic DNA Ladder kit (Chemicon International, Inc., Temecula, CA). The cells seeded on the 12-well plates that were treated with siRNAs as previously mentioned were collected in 1.5-ml microcentrifuge tubes. The cells were washed with PBS, centrifuged, and lysed with 20 μl of TE lysis buffer. The lysates were incubated with 5 μl of enzyme A (RNase A) at 37°C for 10 minutes and then at 55°C for 30 minutes after the addition of 5 μl of Enzyme B (Proteinase K). Afterward, 5 μl of ammonium acetate solution and 100 μl of absolute ethanol were added, and the samples were kept at −20°C for 10 minutes. The samples were centrifuged, and the pellets were washed with 70% ethanol. Then the DNA pellets were dissolved in 30 μl of DNA suspension buffer. DNA fragmentations were visualized by electrophoresis on 2% agarose gel containing ethidium bromide.

Immunohistochemistry

As for positive control, tumor xenograft was made by injection of NB-39-nu cells subcutaneously in 5-week-old SCID mice. Immunohistochemical staining with ALK antibody (αALK) (1:1000), was performed on 16 human neuroblastoma tumors selected from the surgical pathology file at the Department of Pathology, Aichi Medical University based on the results of histopathology evaluation[31] and N-*myc* status. All of those tumor samples were obtained before chemotherapy and irradiation therapy and included nine favorable histology cases with nonamplified N-*myc* (FH&NA), two unfavorable histology cases with amplified N-*myc* (UH&A), and five unfavorable histology cases with nonamplified N-*myc* (UH&NA).

Four-micrometer-thick sections from the formalin-fixed and paraffin-embedded tissue samples were deparaffinized and microwaved for three times for 5 minutes in Na-citrate buffer (pH 6.0) for antigen retrieval. The slides were first immersed in 0.3% hydrogen peroxide in methanol for 20 minutes and then in 10% normal goat serum for 30 minutes. The primary antibody (αALK) was then applied at 4°C overnight, followed by a standard staining procedure using the Vectastain ABC kit (Vector Laboratories, Burlingame, CA). Sections were counterstained with hematoxylin for light microscopic review and evaluation. ALK was always positively detected in the cytoplasm of NB-39-nu tumor xenograft and in the cytoplasm and neuritic processes of normal ganglion cells in the separate positive control sections as well as in the test sections as built-in control, whenever available. As for the negative controls, normal rabbit immunoglobulins (1:500 dilution; Vector Laboratories) or preimmune serum for α ALK (1:1000 dilution) was applied as the primary antibody.

Results

Significant Amplification of the ALK Gene and Constitutive Activation of ALK Kinase in Three Neuroblastoma Cell Lines

As shown in Figure 1A, NB-39-nu, Nagai, and NB-1 cells have significant levels of amplification of the *ALK* gene (30–40 copies per cell) among 25 neuroblastoma and neuroepithelioma cell lines examined. Other cell lines such as SK-N-MC have only one copy of the *ALK* gene just like the

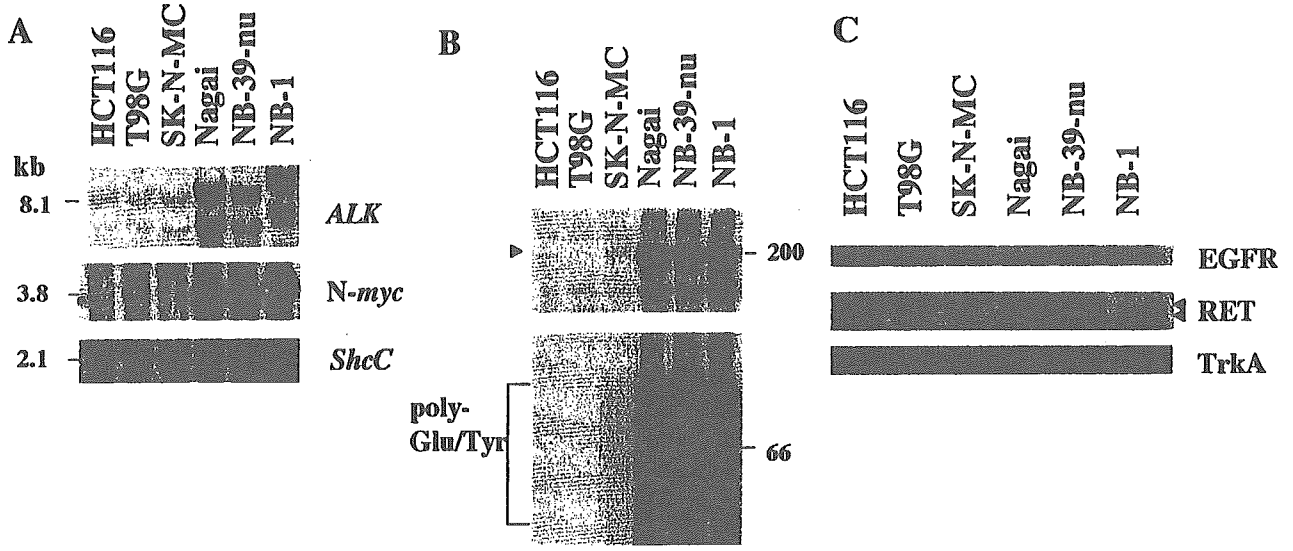

Figure 1. Marked gene amplification of the *ALK* locus and significant elevation of kinase activity of ALK in NB-39-nu, Nagai, and NB-1 cells. **A:** To detect ALK gene amplification, samples of 10 μg of DNA were digested with *Eco*RI. Fragments of about 2.5, 3.1, 6.1, and 8.1 kb were detected using the ^{32}P-labeled probe prepared as previously described.[27] Amplification of the N-*myc* gene was detected using the same filter re-hybridized with the probe for N-*myc*. As a control for the amounts of DNA, the same filter was re-hybridized with the probe for *ShcC*. **B:** *In vitro* kinase assay of ALK in neuroblastoma cells immunoprecipitated with αALK was performed as previously described.[27] Kinase reaction was performed without (**top panel**) or with (**bottom panel**) poly-Glu/Tyr (4:1) as exogenous substrates. Autophosphorylated ALK protein is marked by an **arrow**. Phosphorylated poly-Glu/Tyr is detected as smear indicated by the bracket. **C:** The expression patterns of other receptor tyrosine kinases in neuroblastoma cell lines. Each cell line was harvested, and about 30 μg of whole-cell lysates was subjected to Western blot analysis using the antibodies as indicated on the right. RET proteins are marked by **arrows**.

other types of solid tumor cell lines used as controls. *In vitro* kinase assay revealed outstanding ALK kinase activity in these three cell lines compared with other cells (Figure 1B), which is consistent with our previous study.[27] To examine whether overexpressed and activated ALK affects the expression of other RTKs in these cells, protein expression levels of RTKs, including EGFR, Ret, and TrkA, are compared with other cell lines. Significantly high levels of expression of EGFR and TrkA were observed in two of three cell lines overexpressing ALK (Figure 1C, top and bottom). Ret expression was commonly elevated in all three cell lines with activated ALK, especially in Nagai and NB-39-nu (Figure 1C, middle), consistent with previous study by Northern blotting.[32] Although it is unknown whether overexpression of these RTKs is related to overexpression of ALK, no obvious down-regulation of other RTKs was found in these *ALK*-amplified cell lines.

Inhibition of Activated ShcC, MAPKs, and Akt by Suppressing Activated ALK

To investigate the effect of suppressing the ALK expression level in *ALK*-amplified neuroblastoma cells using the RNAi technique, we synthesized two different RNA duplexes directed against nucleotide positions 153 to 171 and 399 to 417 within coding region *ALK* cDNA (ALK-siRNA1 and ALK-siRNA2, respectively). Because cotransfection of ALK-siRNA1 and ALK-siRNA2 was very effective in suppressing ALK expression, we performed all experiments presented here using a combination of two siRNAs, although similar results were obtained using only ALK-siRNA2. A sequence against the firefly luciferase gene (luc-siRNA) was used as a negative control. The expression of ALK protein is remarkably elevated in NB-39-nu and Nagai compared with other neuroblastoma cell lines, such as SK-M-MC (Figure 2A), caused by gene amplification.[27] The RNA duplexes were transfected into NB-39-nu cells with *ALK* gene amplification and SK-N-MC cells containing only a single copy of the *ALK* gene. We also tried to introduce ALK-siRNAs in several different neuroblastoma cell lines with or without *ALK* amplification in addition to NB-39-nu and SK-N-MC cells, resulting in partial or no reduction of ALK expression presumably due to the unsuccessful introduction in those cells. Therefore, we decided to use these two cell lines to perform further analysis of the effect of ALK knockdown by RNAi technique. RT-PCR analysis revealed that ALK mRNA level was reduced in both NB-39-nu cells and SK-N-MC cells treated with ALK-siRNAs, not in the cells treated with luc-siRNA and s-siRNA (Figure 2B). Both expression and phosphorylation of ALK kinase were significantly suppressed in the NB-39-nu cells treated with ALK-siRNAs compared with a mock-transfection control or cells treated with luc-siRNA (Figure 2C). In these cells, phosphorylation of ShcC was also suppressed despite the unchanged total amount of ShcC (Figure 2C), demonstrating that ShcC is a potent substrate of activated ALK kinase and that activation of ALK is actually responsible for the hyperphosphorylation of ShcC in these cancer cells. While the expression of downstream molecules, such as p44/42 MAPKs and Akt, was not affected by ALK-siRNAs, phosphorylation of these molecules was markedly reduced (Figure 2C). These results suggest that the Ras-MAPK pathway and the phosphatidylinositol 3-kinase/Akt pathway are dominantly regulated by activated ALK kinase in these cells. Interestingly, in SK-N-MC cells treated with ALK-siRNAs, phosphorylation levels of ShcC, p44/42 MAPKs, and Akt were not affected by

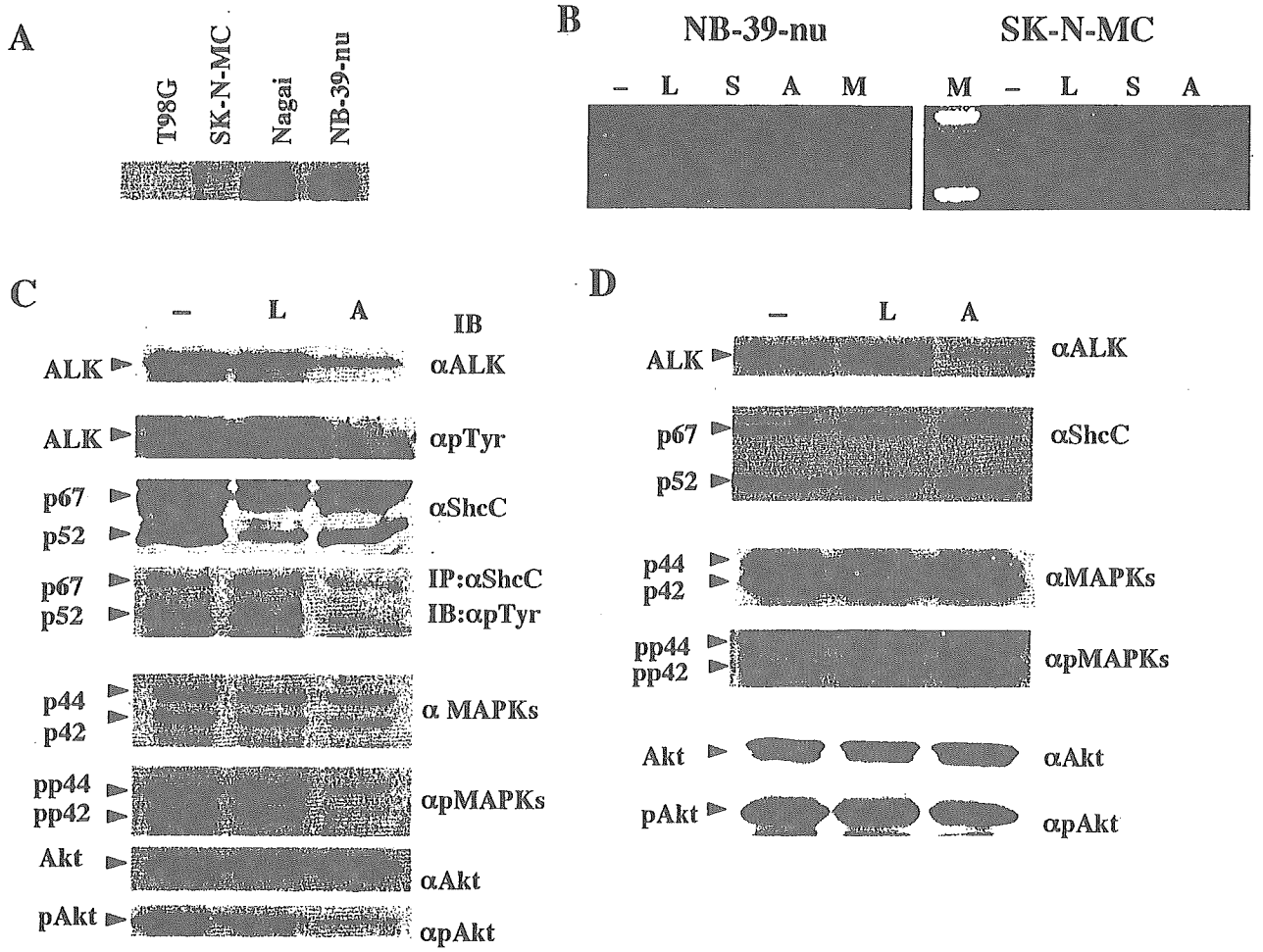

Figure 2. Suppression of ALK expression by siRNAs and changes in downstream molecules NB-39-nu cells and SK-N-MC cells. **A:** Expression levels of ALK protein in neuroblastoma cell lines including NB-39-nu and SK-N-MC. Each cell line was harvested, and about 30 μg of whole-cell lysates was subjected to Western blot analysis using αALK. **B:** mRNA levels of *Alk* in NB-39-nu cells. The cells were lysed at 84 hours after transfection and analyzed by RT-PCR. –, mock transfection; L, cells treated with luc-siRNA; S, cells treated with s-siRNA; A, cells treated with ALK-siRNAs; M, marker. **C:** NB-39-nu cells were harvested 84 hours after transfection. About 10 μg of whole-cell lysates or 250 μg of lysates immunoprecipitated with αShcC was subjected to Western blot analysis using the antibodies as indicated on the right. –, mock transfection; L, cells treated with luc-siRNA; A, cells treated with ALK-siRNAs. **D:** SK-N-MC cells were harvested 48 hours after transfection. About 10 μg of whole-cell lysates was subjected to Western blot analysis using the antibodies as indicated on the right. Bands of ShcC are marked by **arrows**. –, mock transfection; L, cells treated with luc-siRNA; A, cells treated with ALK-siRNAs.

ALK-siRNAs despite further suppression of the basal ALK expression level (Figure 2D), indicating that these pathways are not under the control of ALK in SK-N-MC cells.

Induction of Apoptosis by Suppression of Activated ALK

At 84 hours after transfection, apoptotic morphological changes, such as cell rounding, cytoplasmic blebbing, and irregularities of shape, were observed in NB-39-nu cells treated with ALK-siRNAs, whereas no significant changes were seen in the mock-transfected cells or in the luc-siRNA and the s-siRNA treated cells (Figure 3A). These morphological changes were not observed in SK-N-MC cells treated with ALK-siRNAs (data not shown). At 90 hours after transfection, NB-39-nu cells treated with ALK-siRNAs started to detach from the dish due to cell death.

To examine the localization of expression of ALK kinase, we performed double staining by anti-ALK antibody and TOTO-3, which stains the nucleus, in several neuroblastic cell lines. As shown in Figure 1D, unexpectedly, ALK protein overexpressed in NB-39-nu cells is localized in both membrane and cytoplasm. ALK staining was very weak in cell lines such as YT-nu and SK-N-MC with one copy of the *ALK* gene, however, its localization appeared to be the same as in NB-39-nu (data not shown). It was observed that the expression of ALK was completely lost after the RNAi-induced suppression of ALK (Figure 3C, top). To confirm whether the cell death resulted from apoptosis, cells were also analyzed by immunofluorescent TUNEL staining in NB-39-nu cells. TUNEL staining was clearly positive in these cells at 84 hours after transfection (Figure 3C, middle), indicating that apoptosis was induced in NB-39-nu cells treated with ALK-siRNAs. No significant TUNEL staining was observed in the mock-transfected cells or the luc-siRNA treated cells. Finally, DNA fragmentation assay was performed to measure the endonuclease activity accompa-

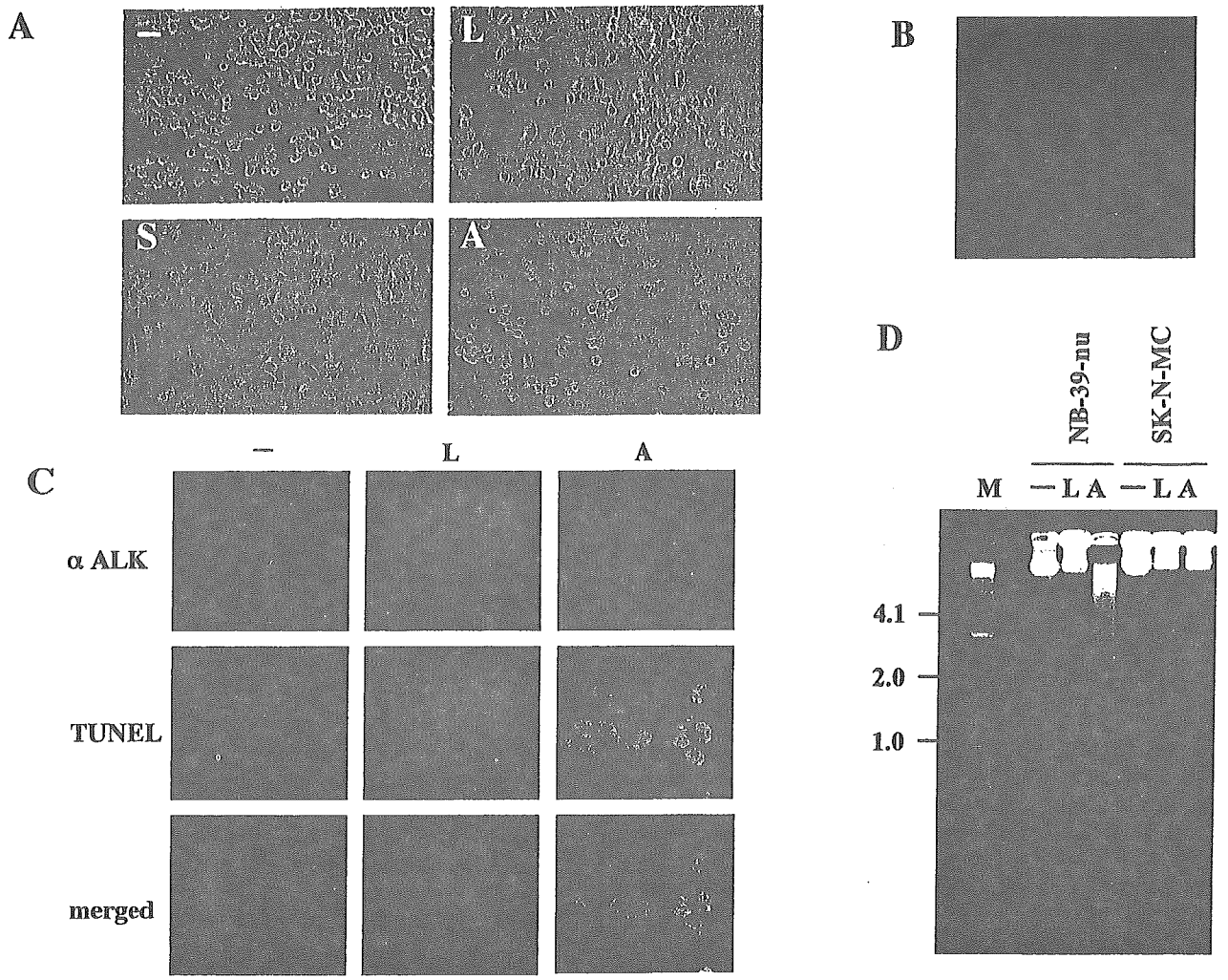

Figure 3. Induction of apoptosis in NB-39-nu cells treated with ALK-siRNAs. **A:** NB-39-nu cells on the dish were observed 84 hours after transfection under a light microscope. −, mock transfection; L, cells treated with luc-siRNA; S, cells treated with s-siRNA; A, cells treated with ALK-siRNAs. **B:** Cytoplasmic expression of ALK by immunocytostaining. The cells were stained for the expression of ALK (red) and apoptotic cells by TOTO-3 (blue). **C:** Cells on 24-well plates were fixed, and TUNEL assay was followed by staining with αALK (GST). The cells were stained for the expression of ALK (red) and apoptotic cells by TUNEL (green). −, mock transfection; L, cells treated with luc-siRNA; A, cells treated with ALK-siRNAs. **D:** DNA fragmentation assay in NB-39-nu cells and SK-N-MC cells treated with siRNAs. Genomic DNA was extracted 84 hours and 48 hours after transfection in NB-39-nu and in SK-N-MC, respectively. They were analyzed using electrophoresis. −, mock transfection; L, cells treated with luc-siRNA; A, cells treated with ALK-siRNAs; M, marker.

nied by apoptosis. The formation of significant DNA fragmentation was observed in the NB-39-nu cells but not in SK-N-MC cells treated with ALK-siRNAs (Figure 3D), indicating that cell apoptosis was induced through the suppression of ALK only in the NB-39-nu cells. This suggests that signaling pathways downstream of activated ALK dominantly regulate the survival of neuroblastoma cells with amplified ALK; therefore, the loss of ALK protein results in apoptotic changes to these cells.

Expression of ALK in Primary Neuroblastoma Tissues

Immunohistochemically, ALK was positively detected both in the cytoplasm of the neuroblastic cells and in the fine meshwork of neuropil of seven of nine tumors with favorable histology cases with nonamplified *N-myc* (FH&NA) (Figure 4, B and C). All seven unfavorable histology tumors (two UH&A tumors and five UH&NA tumors) were positive in the cytoplasm and/or in the fine meshwork of neuropil for ALK (Figure 4A). There was no correlation between the frequency or intensity of ALK-staining and histology of neuroblastoma tissues, showing majority of neuroblastoma samples showed a detectable amount of ALK. There was no significant staining using preimmune serum from the same rabbit as that for anti-ALK antibody (data not shown). Essentially the same results were obtained using a mouse monoclonal antibody against human ALK (ALK1: DAKO) (data not shown).

Amplification of the ALK Gene in Primary Neuroblastoma Tissues

It is essential to show whether ALK overexpression or gene amplification occurs in actual human neuroblastoma tissues in addition to neuroblastoma cell lines.

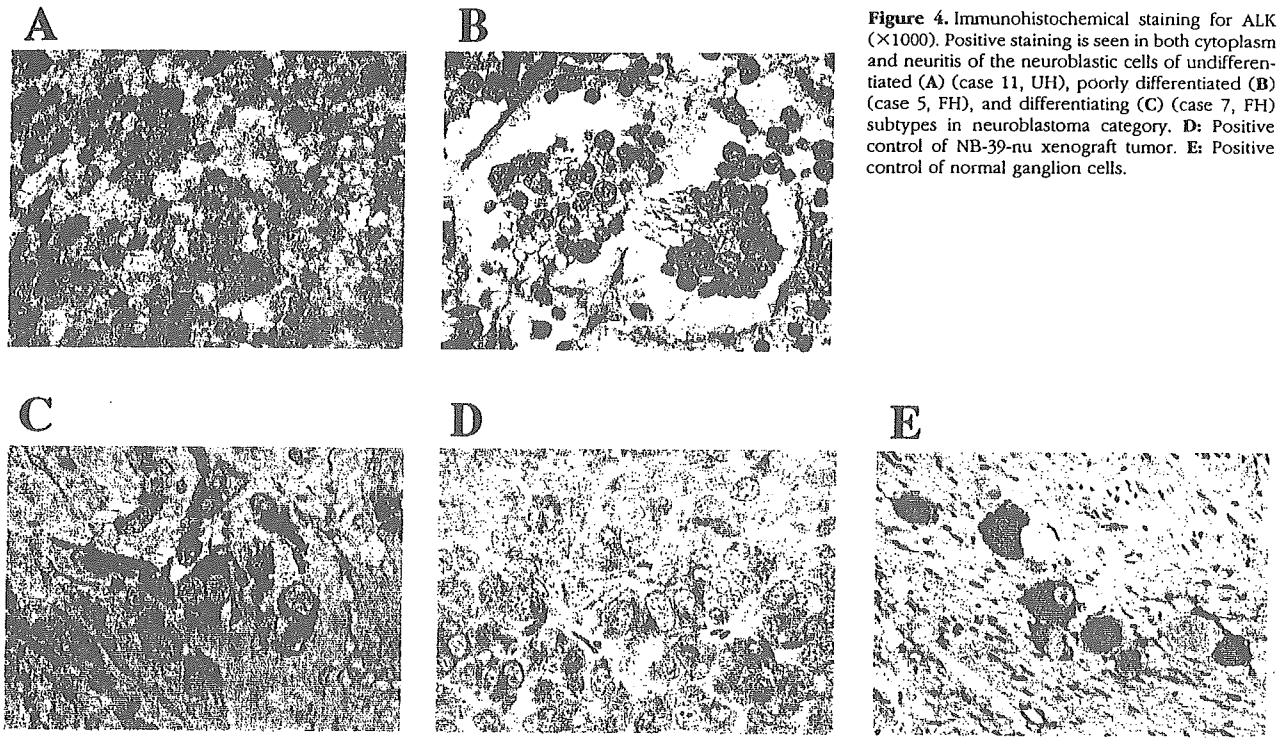

Figure 4. Immunohistochemical staining for ALK (×1000). Positive staining is seen in both cytoplasm and neuritis of the neuroblastic cells of undifferentiated (**A**) (case 11, UH), poorly differentiated (**B**) (case 5, FH), and differentiating (**C**) (case 7, FH) subtypes in neuroblastoma category. **D:** Positive control of NB-39-nu xenograft tumor. **E:** Positive control of normal ganglion cells.

Therefore, the mRNA amount of ALK kinase was first examined by RT-PCR on 32 primary neuroblastoma tissues (16 tissues with N-*myc* amplification and 16 tissues without N-*myc* amplification). Two of 32 cases showed slight elevation of *ALK* mRNA expression using several primer sets beyond the average expression level (data not shown).

To obtain more precise information about the copy numbers of *ALK*, we next analyzed the genomic DNAs of primary neuroblastoma tissues using Southern blot analysis. Whole purified DNA samples of tumors from 85 patients were examined. About the same number of N-*myc*-positive and N-*myc*-negative samples were collected to examine the relation between *Alk* and N-*myc* amplification. The intensities of signals on Southern blot membranes corresponding to the *ALK* gene and control *ShcC* gene, which is located on 9q22, were measured using a Molecular Imager FxPro (Bio-Rad), and the ratio of *ALK* signals to *ShcC* signals was calculated for each sample. Because more than 80% (70 samples) showed consistent ratios with each other in each experiment, these samples are treated as putative "single copy" controls. As several other samples showed apparently elevated intensity ratios, suggesting *ALK* amplification, relative copy numbers of *ALK* were calculated in comparison with average intensity ratios of putative single copy controls in each experiment. The results showed that there was significant *ALK* gene amplification in 8 of 85 patients (9.4%) (Figure 5). Seven of these eight cases, however, had only 1.8 to 3.0 copies of the *ALK* gene, suggesting a moderate gain of chromosomal focus rather than severe amplification. There was only one case that had outstanding amplification of ALK with approximately 10 copies. N-*myc* gene amplification was also detected in this case. The characteristics of the eight patients with *ALK* gain or amplification are shown in Table 1. Whereas seven of eight patients were classified as Stage III or IV (one as Stage III and six as Stage IV), the rest was classified as Stage I. The case with *ALK* amplification had N-*myc* amplification and was classified as Stage IV. Seven of eight patients were more than 1 year of age.

Discussion

Studies on ALK kinase demonstrate that activated ALK is involved in malignant tumor formation as forms of fusion proteins that force oligomerization of this kinase. We recently showed that the intact form of ALK protein is con-

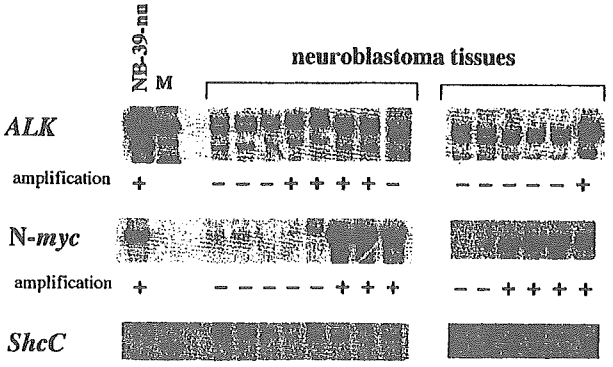

Figure 5. Detection of gene amplification of *ALK* and N-*myc* in primary neuroblastoma tissues. *ALK* was amplified in eight cases, and five of these eight cases are shown. The probe for *ALK* was removed from the filters, and the filters were re-hybridized in turn with other probes. Of eight cases with *ALK* amplification, N-*myc* amplification was detected in six cases and not detected in two cases. The probe for *ShcC* was used as a control for the amounts of DNA. M, marker.

stitutively activated by *ALK* gene amplification in three neuroblastoma cell lines, indicating a novel mechanism of activation of ALK kinase in malignancies.[27] In this study, amplification of the *ALK* gene was detected in primary neuroblastoma tissues for the first time. This suggests that activated ALK kinase plays a real role in the pathophysiology of neuroblastoma, such as giving a more malignant phenotype to the tumors by perturbing signal transduction. Recently, Motegi et al[33] showed that ALK transmits both mitogenic and differentiation signals, and that the MAPK pathway plays an important role in these effects in SK-N-SH cells without *ALK* gene amplification. Together with the fact that activated ALK surpasses regulation by other RTKs in cell lines with *ALK* gene amplification,[27] our new results showing apoptotic changes caused by the suppression of activated ALK protein clearly demonstrate the dominant role of ALK kinase in the survival of the *ALK*-amplified type of neuroblastoma.

The frequency and copy numbers of gene amplification of ALK were significantly lower in neuroblastic tumors compared with neuroblastic cell lines. Remarkable amplification of the *ALK* gene was detected in 1 tumor tissue of 85 tumor samples examined. Three neuroblastoma cell lines with *ALK* amplification had more than 30 copies of *ALK*, whereas primary neuroblastoma containing *ALK* gene amplification had within a range of 2 to 10 copies. This may be due to underestimation of the copy number in the tumor cells because of contamination of stromal cells and lymphocytes into the tumor tissues.[34,35] There may also be a mechanism in which cells with a higher copy number of *ALK* become the major population during the establishment of cell lines because of their growth advantage. Immunohistochemical analysis demonstrated, however, universal cytoplasmic expression of ALK in a wide range of neuroblastoma tumor samples, suggesting some transcriptional or posttranslational regulation of the ALK amount might exist in neuroblastoma cells. Although, due to the condition of the samples, we were unable to obtain information on the copy numbers of the *ALK* gene as for the samples used in the immunohistochemical analysis, further immunohistochemical screening may reveal neuroblastoma tissues with an outstanding amount of ALK protein because of gene amplification.

The N-*myc* gene was also amplified in this tumor and in all three cell lines with *ALK* amplification (NB-39-nu, Nagai, and NB-1). N-*myc* is located on 2p24.3 and *ALK* is on 2p23.2, suggesting that there is a tendency to synchronic amplification between N-*myc* and *ALK*. We were unable to conclude that there was an association between ALK amplification and prognosis mainly due to the limited number of positive samples and the short-term follow-up. Moreover, the *ALK* gene locus appears too far from the N-*myc* gene locus to be within a single amplicon. Further analysis in a greater number of samples with longer follow-up is necessary.

The activation of ALK results in hyperphosphorylation of ShcC in neuroblastoma cells, and NB-39-nu cells treated with ALK-siRNAs show suppressed tyrosine phosphorylation of ShcC, followed by apoptotic changes to these cells, suggesting that ShcC is a physiological substrate of the activated ALK kinase and that the ALK-ShcC pathway dominantly controls the survival of NB-39-nu cells even with the existence of other RTKs, such as EGFR, TrkA, and Ret. In neuronal cells, both ShcB (Sli/SCK) and ShcC (Rai/N-Shc) can bind activated RTKs, including the EGFR and Trk receptor.[36–39] Mice lacking both ShcB and ShcC exhibit a significant loss of sympathetic neurons, suggesting that ShcB and ShcC act in supporting sympathetic development and survival.[28] A recent study also showed that ShcC is a physiological substrate of Ret kinase and that it exerts a prosurvival function in neuronal cells.[40] Although high levels of TrkA expression correlate with a favorable outcome of neuroblastoma patients,[20] TrkA expression was significantly high in NB-39-nu and Nagai, which derive from tumors with a poor prognosis. This discrepancy may also be explained by the overwhelming control of cell survival by ALK kinase in these cell lines. Neuronal apoptosis is regulated through the action of critical protein kinase cascades, such as the phosphatidylinositol 3-kinase/Akt pathway and the Ras-MAPK pathway.[41,42] Apparently, neither pathway is properly controlled by EGF or nerve growth factor in NB-39-nu cells or Nagai cells.[27] Here, we also demonstrated that the suppression of activated ALK blocks MAPKs and Akt in these cells, resulting in apoptosis. On the other hand, the activity of MAPKs and Akt was not reduced by the suppression of a single copy of *ALK* in SK-N-MC cells. These results suggest that activation of ALK kinase completely remodeled the cellular signaling transduction pathways through ShcC so that cell survival entirely depended on signals originating from ALK kinase.

In conclusion, phosphorylation of several signaling molecules and cancer survival might be under the control of activated ALK kinase when gene amplification of ALK is as significant as in NB-39-nu cells, although the frequency of gene amplification in neuroblastoma tissues is not high. Cytoplasmic expression of ALK in neuroblastoma cells may suggest distinct function of this kinase in cell proliferation and survival. These findings further suggest that activated ALK kinase will be indispensable information for prognosis and treatment of neuroblastoma although the frequency is low.

References

1. Ullrich A, Schlessinger J: Signal transduction by receptors with tyrosine kinase activity. Cell 1990, 61:203–212
2. Heldin CH: Dimerization of cell surface receptors in signal transduction. Cell 1995, 80:213–223
3. Blume-Jensen P, Hunter T: Oncogenic kinase signalling. Nature 2001, 411:355–365
4. Pawson T: Protein modules and signalling networks. Nature 1995, 373:573–580
5. Kozlowski M, Larose L, Lee F, Le DM, Rottapel R, Siminovitch KA: SHP-1 binds and negatively modulates the c-Kit receptor by interaction with tyrosine 569 in the c-Kit juxtamembrane domain. Mol Cell Biol 1998, 18:2089–2099
6. Morris SW, Kirstein MN, Valentine MB, Dittmer KG, Shapiro DN, Saltman DL, Look AT: Fusion of a kinase gene ALK, to a nucleolar protein gene NPM, in non-Hodgkin's lymphoma. Science 1994, 263:1281–1284

7. Shiota M, Fujimoto J, Semba T, Satoh H, Yamamoto T, Mori S: Hyperphosphorylation of a novel 80 kDa protein-tyrosine kinase similar to Ltk in a human Ki-1 lymphoma cell line, AMS3. Oncogene 1994, 9:1567–1574
8. Bridge JA, Kanamori M, Ma Z, Pickering D, Hill DA, Lydiatt W, Lui MY, Colleoni GW, Antonescu CR, Ladanyi M, Morris SW: Fusion of the ALK gene to the clathrin heavy chain gene, CLTC, in inflammatory myofibroblastic tumor. Am J Pathol 2001, 159:411–415
9. Iwahara T, Fujimoto J, Wen D, Cupples R, Bucay N, Arakawa T, Mori S, Ratzkin B, Yamamoto T: Molecular characterization of ALK, a receptor tyrosine kinase expressed specifically in the nervous system. Oncogene 1997, 14:439–449
10. Morris SW, Naeve C, Mathew P, James PL, Kirstein MN, Cui X, Witte DP: ALK, the chromosome 2 gene locus altered by the t(2;5) in non-Hodgkin's lymphoma, encodes a novel neural receptor tyrosine kinase that is highly related to leukocyte tyrosine kinase (LTK). Oncogene 1997, 14:2175–2188
11. Ben-Neriah Y, Bauskin AR: Leukocytes express a novel gene encoding a putative transmembrane protein-kinase devoid of an extracellular domain. Nature 1988, 333:672–676
12. Maru Y, Hirai H, Takaku F: Human Itk: gene structure and preferential expression in human leukemic cells. Oncogene Res 1990, 5:199–204
13. Bernards A, de la Monte SM: The Itk receptor tyrosine kinase is expressed in pre-B lymphocytes and cerebral neurons and uses a non-AUG translational initiator. EMBO J 1990, 9:2279–2287
14. Pulford K, Lamant L, Morris SW, Butler LH, Wood KM, Stroud D, Delsol G, Mason DY: Detection of anaplastic lymphoma kinase (ALK) and nucleolar protein nucleophosmin (NPM)-ALK proteins in normal and neoplastic cells with the monoclonal antibody ALK1. Blood 1997, 89:1394–1404
15. Shiota M, Fujimoto J, Takenaga M, Satoh H, Ichinohasama R, Abe M, Nakano M, Yamamoto T, Mori S: Diagnosis of t(2;5)(p23;q35)-associated Ki-1 lymphoma with immunohistochemistry. Blood 1994, 84:3648–3652
16. Duyster J, Bai RY, Morris SW: Translocations involving anaplastic lymphoma kinase (ALK). Oncogene 2001, 20:5623–5637
17. Stoica GE, Kuo A, Aigner A, Sunitha I, Souttou B, Malerczyk C, Caughey DJ, Wen D, Karavanov A, Riegel AT, Wellstein A: Identification of anaplastic lymphoma kinase as a receptor for the growth factor pleiotrophin. J Biol Chem 2001, 276:16772–16779
18. Stoica GE, Kuo A, Powers C, Bowden ET, Sale EB, Riegel AT, Wellstein A: Midkine binds to anaplastic lymphoma kinase (ALK) and acts as a growth factor for different cell types. J Biol Chem 2002, 277:35990–35998
19. Evans AE, D'Angio GJ, Randolph J: A proposed staging for children with neuroblastoma: children's cancer study group A. Cancer 1971, 27:374–378
20. Nakagawara A, Arima-Nakagawara M, Scavarda NJ, Azar CG, Cantor AB, Brodeur GM: Association between high levels of expression of the TRK gene and favorable outcome in human neuroblastoma. N Engl J Med 1993, 328:847–854
21. Nakagawara A, Azar CG, Scavarda NJ, Brodeur GM: Expression and function of TRK-B and BDNF in human neuroblastomas. Mol Cell Biol 1994, 14:759–767
22. Nakagawara A, Nakamura Y, Ikeda H, Hiwasa T, Kuida K, Su MS, Zhao H, Cnaan A, Sakiyama S: High levels of expression and nuclear localization of interleukin-1 beta converting enzyme (ICE) and CPP32 in favorable human neuroblastomas. Cancer Res 1997, 57:4578–4584
23. Posmantur R, McGinnis K, Nadimpalli R, Gilbertsen RB, Wang K: Characterization of CPP32-like protease activity following apoptotic challenge in SH-SY5Y neuroblastoma cells. J Neurochem 1997, 68:2328–2337
24. Adida C, Berrebi D, Peuchmaur M, Reyes-Mugica M, Altieri DC: Anti-apoptosis gene, survivin, and prognosis of neuroblastoma. Lancet 1998, 351:882–883
25. Hiyama E, Hiyama K, Yokoyama T, Matsuura Y, Piatyszek MA, Shay JW: Correlating telomerase activity levels with human neuroblastoma outcomes. Nat Med 1995, 1:249–255
26. Lamant L, Pulford K, Bischof D, Morris SW, Mason DY, Delsol G, Mariame B: Expression of the ALK tyrosine kinase gene in neuroblastoma. Am J Pathol 2000, 156:1711–1721
27. Miyake I, Hakomori Y, Shinohara A, Gamou T, Saito M, Iwamatsu A, Sakai R: Activation of anaplastic lymphoma kinase is responsible for hyperphosphorylation of ShcC in neuroblastoma cell lines. Oncogene 2002, 21:5823–5834
28. Sakai R, Henderson JT, O'Bryan JP, Elia AJ, Saxton TM, Pawson T: The mammalian ShcB and ShcC phosphotyrosine docking proteins function in the maturation of sensory and sympathetic neurons. Neuron 2000, 28:819–833
29. Perucho M, Goldfarb M, Shimizu K, Lama C, Fogh J, Wigler M: Human-tumor-derived cell lines contain common and different transforming genes. Cell 1981, 27:467–476
30. Brodeur GM, Pritchard J, Berthold F, Carlsen NL, Castel V, Castelberry RP, De Bernardi B, Evans AE, Favrot M, Hedborg F, Kaneko M, Kemshead J, Lampert F, Lee RE, Look AT, Pearson AD, Philip T, Roald B, Sawada T, Seeger RC, Tsuchida Y, Voute PA: Revisions of the international criteria for neuroblastoma diagnosis, staging, and response to treatment. J Clin Oncol 1993, 11:1466–1477
31. Shimada H, Ambros IM, Dehner LP, Hata J, Joshi VV, Roald B, Stram DO, Gerbing RB, Lukens JN, Matthay KK, Castleberry RP: The International Neuroblastoma Pathology Classification (the Shimada system). Cancer 1999, 86:364–372
32. Ikeda I, Ishizaka Y, Tahira T, Suzuki T, Onda M, Sugimura T, Nagao M: Specific expression of the ret proto-oncogene in human neuroblastoma cell lines. Oncogene 1990, 5:1291–1296
33. Motegi A, Fujimoto J, Kotani M, Sakuraba H, Yamamoto T: ALK receptor tyrosine kinase promotes cell growth and neurite outgrowth. J Cell Sci 2004, 117:3319–3329
34. Slamon DJ, Clark GM, Wong SG, Levin WJ, Ullrich A, McGuire WL: Human breast cancer: correlation of relapse and survival with amplification of the HER-2/neu oncogene. Science 1987, 235:177–182
35. Tsuda H, Hirohashi S, Shimosato Y, Hirota T, Tsugane S, Yamamoto H, Miyajima N, Toyoshima K, Yamamoto T, Yokota J, Yoshida T, Sakamoto H, Terada M, Sugimura T: Correlation between long-term survival in breast cancer patients and amplification of two putative oncogene-coamplification units: hst-1/int-2 and c-erbB-2/ear-1. Cancer Res 1989, 49:3104–3108
36. Ganju P, O'Bryan JP, Der C, Winter J, James IF: Differential regulation of SHC proteins by nerve growth factor in sensory neurons and PC12 cells. Eur J Neurosci 1998, 10:1995–2008
37. Nakamura T, Komiya M, Gotoh N, Koizumi S, Shibuya M, Mori N: Discrimination between phosphotyrosine-mediated signaling properties of conventional and neuronal Shc adapter molecules. Oncogene 2002, 21:22–31
38. Nakamura T, Muraoka S, Sanokawa R, Mori N: N-Shc and Sck, two neuronally expressed Shc adapter homologs: their differential regional expression in the brain and roles in neurotrophin and Src signaling. J Biol Chem 1998, 273:6960–6967
39. O'Bryan JP, Songyang Z, Cantley L, Der CJ, Pawson T: A mammalian adaptor protein with conserved Src homology 2 and phosphotyrosine-binding domains is related to Shc and is specifically expressed in the brain. Proc Natl Acad Sci USA 1996, 93:2729–2734
40. Pelicci G, Troglio F, Bodini A, Melillo RM, Pettirossi V, Coda L, De Giuseppe A, Santoro M, Pelicci PG: The neuron-specific Rai (ShcC) adaptor protein inhibits apoptosis by coupling Ret to the phosphatidylinositol 3-kinase/Akt signaling pathway. Mol Cell Biol 2002, 22:7351–7363
41. Yuan J, Yankner BA: Apoptosis in the nervous system. Nature 2000, 407:802–809
42. De Vita G, Melillo RM, Carlomagno F, Visconti R, Castellone MD, Bellacosa A, Billaud M, Fusco A, Tsichlis PN, Santoro M: Tyrosine 1062 of RET-MEN2A mediates activation of Akt (protein kinase B) and mitogen-activated protein kinase pathways leading to PC12 cell survival. Cancer Res 2000, 60:3727–3731

LMO3 Interacts with Neuronal Transcription Factor, HEN2, and Acts as an Oncogene in Neuroblastoma

Mineyoshi Aoyama,[1] Toshinori Ozaki,[1] Hiroyuki Inuzuka,[1] Daihachiro Tomotsune,[3] Junko Hirato,[4] Yoshiaki Okamoto,[1] Hisashi Tokita,[2] Miki Ohira,[1] and Akira Nakagawara[1]

Divisions of [1]Biochemistry and [2]Animal Science, Chiba Cancer Center Research Institute; [3]Center for Functional Genomics, Hisamitsu Pharmaceutical Co., Inc., Chiba, Japan and [4]Department of Pathology, Gunma University School of Medicine, Gunma, Japan

Abstract

LIM-only proteins (LMO), which consist of LMO1, LMO2, LMO3, and LMO4, are involved in cell fate determination and differentiation during embryonic development. Accumulating evidence suggests that LMO1 and LMO2 act as oncogenic proteins in T-cell acute lymphoblastic leukemia, whereas LMO4 has recently been implicated in the genesis of breast cancer. However, little is known about the role of LMO3 in either tumorigenesis or development. In the present study, we have identified *LMO3* and *HEN2*, which encodes a neuronal basic helix-loop-helix protein, as genes whose expression levels were higher in unfavorable neuroblastomas compared with those of favorable tumors. Immunoprecipitation and immunostaining experiments showed that LMO3 was associated with HEN2 in mammalian cell nucleus. Human neuroblastoma SH-SY5Y cells stably overexpressing LMO3 showed a marked increase in cell growth, a promotion of colony formation in soft agar medium, and a rapid tumor growth in nude mice compared with the control transfectants. More importantly, the increased expression of LMO3 and HEN2 was significantly associated with a poor prognosis in 87 primary neuroblastomas. These results suggest that the deregulated expression of neuronal-specific LMO3 and HEN2 contributes to the genesis and progression of human neuroblastoma in a lineage-specific manner. (Cancer Res 2005; 65(11): 4587-97)

Introduction

The LIM domain–containing proteins are important regulators in determining cell fate and controlling cell growth and differentiation during embryonic development (1). The LIM domain is a highly conserved cysteine-rich zinc finger–like motif found in a variety of nuclear and cytoplasmic proteins and acts as a docking site for the assembly of multiprotein complexes (2–4). However, the precise role of the LIM domain is still unclear. Several distinct subgroups of the LIM domain–containing proteins are defined and some of them also possess a functionally divergent domain, including a DNA-binding homeodomain or a protein kinase domain (1, 2).

The LIM-only proteins (LMO) are one of the families of the LIM domain–containing proteins and possess only two tandem LIM domains. They consist of four members, including LMO1, LMO2, LMO3, and LMO4 (2, 4). *LMO1* and *LMO2* have been identified as the genes that are activated in human acute T-cell leukemia (T-cell ALL) by tumor-specific chromosomal translocations (4). Transgenic mice overexpressing LMO1 or LMO2 developed immature and aggressive T-cell leukemia, suggesting that these proteins act as T-cell oncoproteins (5–7). On the other hand, LMO4 has been identified as a nuclear protein that interacts with the adaptor protein Ldb1 (8). It has been shown recently that LMO4 is highly expressed in primary human breast cancers, and overexpression of LMO4 inhibits differentiation of mammary epithelial cells, suggesting that deregulated expression of LMO4 contributes to the breast carcinogenesis (9). LMO4 has also been reported to be associated with BRCA1 to repress its transcriptional activity (10). Thus, LMO1, LMO2, and LMO4 have been implicated in tumorigenesis. However, to date, little is known about the oncogenic function of LMO3, which has been discovered based on sequence homology with LMO1 (11).

The nuclear LMO proteins, which lack intrinsic DNA-binding activity, have been considered to be involved in transcriptional regulation (2), raising a possibility that they alter the transcription of target genes by forming a complex with other transcription factors with DNA-binding activity. Indeed, in T-cell acute lymphoblastic leukemia in children, a basic helix-loop-helix transcription factor, TAL1, is physically associated with LMO1 or LMO2 and enhances their oncogenic activities (12, 13). Interestingly, the neuronal-specific basic helix-loop-helix transcription factors, HEN1 and HEN2, were identified based on cross-hybridization with TAL1 (14, 15). Their expression was restricted to the developing nervous system and a human neuroblastoma cell line. However, the role of HEN1 and HEN2 in tumorigenesis has long been elusive.

Neuroblastoma is one of the most common childhood cancers and is originated from sympathoadrenal lineage of the neural crest (16). It is clinically and cytogenetically divided into two major subgroups with favorable and unfavorable prognosis (17). The recent molecular and cellular analyses have revealed that amplification of *MYCN* and *DDX1* as well as loss of heterozygosity at the region of chromosome 1p36 are strongly associated with a poor outcome, whereas high levels of expression of the neurotrophin receptors *TrkA*, *CD44*, and *Fyn*, are well correlated with favorable prognosis (16–23). However, we still do not know many other genes that play important roles in the genesis and progression of neuroblastoma. To identify the other genes closely involved in neuroblastoma, we have constructed several cDNA libraries from different subsets of neuroblastoma and randomly cloned 4,200 genes (24). Screening of the genes differentially expressed between favorable and unfavorable subsets of the tumor has identified *Nbla3267* as one of the genes expressed at higher levels in unfavorable than favorable neuroblastomas (25).

In the present study, we found that *Nbla3267* encoded the human LMO, LMO3, and that high expression of *LMO3* as well as *HEN2* was strongly associated with a poor prognosis of neuroblastoma. Furthermore, LMO3 interacted with HEN2 in mammalian

Requests for reprints: Akira Nakagawara, Division of Biochemistry, Chiba Cancer Center Research Institute, 666-2 Nitona, Chuoh-ku, Chiba 260-8717, Japan. Phone: 81-43-264-5431; Fax: 81-43-265-4459; E-mail: akiranak@chiba-cc.jp.

cell nucleus, and enforced expression of LMO3 in human neuroblastoma-derived cell line SH-SY5Y markedly enhanced tumor growth in nude mice, supporting the oncogenic role of LMO3 in neuroblastoma.

Materials and Methods

Patient population. The RNA samples obtained from 87 patients with neuroblastoma were subjected to semiquantitative and quantitative real-time reverse transcription-PCR (RT-PCR) analyses. All patients were diagnosed clinically as well as pathologically and tested for DNA ploidy, MYCN amplification, and TrkA expression. Tumors were staged according to the International Neuroblastoma Staging System criteria (26). Thirty-four patients were stage I, 14 were stage II, 8 were stage III, 26 were stage IV, and 5 were stage IVS. Stages I, II, and IVS were considered as favorable and stages III and IV as unfavorable. The patients were treated following the protocols proposed by the Japanese Infantile Neuroblastoma Cooperative Study (27) and the Study Group of Japan for Treatment of Advanced Neuroblastoma (28). The clinical follow-up ranged from 4 to 58 months, with a median of 36 months. We have a precise list of patient characteristics, including age, stage, and clinical follow-up time, and this list will be provided upon request.

Cloning of human *LMO3*, *HEN1*, and *HEN2*. To obtain a complete human *LMO3* cDNA, a cDNA library derived from human fetal brain (Stratagene, La Jolla, CA) was screened with a ^{32}P-labeled *Nbla3267* cDNA. Plaques showing positive signals were picked up and rescreened twice. To construct the expression plasmid for hemagglutinin (HA)–tagged LMO3-A, the cDNA fragment encoding the entire LMO3-A protein was amplified by PCR from the phage clone as a template using the primers designed to add a synthetic linker encoding the HA epitope on the NH_2-terminal side of LMO3-A (forward 5′-GGTACCATGGCTTACCCATACGATGTTCCA-GATTACGCTAGCCTCTCAGTCCAGCCAGACAC-3′ and reverse 5′-TCAGA-TATCATTAGATCAGCGAACCTGGG-3′). The PCR product was digested with *Kpn*I and *Eco*RV and subcloned into the identical restriction sites of pcDNA3 expression plasmid to give pcDNA3-HA-LMO3-A. cDNA encoding human HEN1 (amino acid residues 1-133) or HEN2 (amino acid residues 1-135) was generated by reverse transcribing total RNA isolated from neuroblastoma cell line, IMR32, using a forward primer (5′-AAGGAATTCATGCTCAACTCAGACACCATG-3′) and a reverse primer (5′-ATAAGAATGCGGCCGCTCAGACGT-3′) for HEN1 and a forward primer (5′-AAGGAATTCATGCTGAGTCCGGACCAAGCA-3′) and a reverse primer (5′-ATAAGAATGCGGCCGCCTACACGTCCAGGACGTGGTT-3′) for HEN2. The amplified PCR products were digested with *Eco*RI and *Not*I and subcloned into the identical restriction sites of pcDNA3-FLAG expression plasmid to give pcDNA-FLAG-HEN1 and pcDNA3-FLAG-HEN2.

Generation of a polyclonal anti-LMO3 antibody. The polyclonal anti-LMO3 and anti-HEN2 antibodies were raised against a peptide "Cys" plus containing the amino acid sequence between positions 127 and 145 of LMO3 and the amino acid sequence between positions 1 and 19 of HEN2, respectively. The peptides and the polyclonal antibodies were produced by Biologica Co. (Nagoya, Japan).

Cell culture and transfection. Human neuroblastoma (SK-N-AS, SH-SY5Y, NB69, OAN, SK-N-BE, NGP, NLF, IMR32, NB1, and KP-N-NS), ALL (RPMI, KOPT, HSB, and MOLT), osteosarcoma (OST, SAOS-2, and U2OS), rhabdomyosarcoma (RMS-MK), colon cancer (COLO-320), breast cancer (MCF-7 and MDA-MB-453), melanoma (G361, G32TG, and A875), thyroid cancer (TTC11), small cell lung carcinoma (H1299), and cervical cancer (HeLa) cell lines and COS7 cells were maintained in RPMI 1640 or DMEM supplemented with 10% heat-inactivated fetal bovine serum (FBS), 100 IU/mL penicillin, and 100 μg/mL streptomycin at 37°C in an atmosphere of 5% CO_2 in the air. For transient transfection, COS7 cells were transfected with the indicated expression plasmids using FuGene 6 transfection reagent as recommended by the manufacturer (Roche Molecular Biochemicals, Mannheim, Germany). Stable transfections of SH-SY5Y cells were done with the empty plasmid (pcDNA3, Invitrogen, Carlsbad, CA) or with the expression plasmid for FLAG-tagged LMO3-A using LipofectAMINE Plus transfection reagent according to the manufacturer's instructions (Invitrogen). The transfected cells were cultured in the presence of G418 at a final concentration of 400 μg/mL (Sigma Chemical Co., St. Louis, MO). Thereafter, the selection medium was replaced every 3 days. Three weeks after the selection in G418, drug-resistant clones were isolated and allowed to proliferate in medium containing G418.

Reverse transcription-PCR analysis. Total RNA was prepared from cultured cells and human tissues by using Trizol reagent (Life Technologies, Grand Island, NY) or the RNeasy Mini kit (Qiagen, Valencia, CA). Reverse transcription was carried out using random primers and SuperScript II (Invitrogen). Following the reverse transcription, the resultant cDNA was subjected to PCR-based amplification. Oligonucleotides used to amplify *LMO3-A*, *LMO3-B*, *LMO1*, *LMO2*, *LMO4*, *Ldb1*, *Ldb2*, *TAL1*, *HEN1*, *HEN2*, and glyceraldehyde-3-phosphate dehydrogenase (*GAPDH*) mRNAs were as follows: *LMO3-A*: forward 5′-ACTGTGCTTACTGAACGGCCTC-3′ and reverse 5′-CCGGTCCTTGATCTTTCGGTTG-3′; *LMO3-B*: forward 5′-TGCAACTCA-GACACGCCTAAG-3′ and reverse 5′-CCGGTCCTTGATCTTTCGGTTG-3′; *LMO1*: forward 5′-GCTCCACCCTCTACACCAAG-3′ and reverse 5′-CTGCCCTTCCTCATAGTCCA-3′; *LMO2*: forward 5′-AATGCGGGTGAAAGA-CAAAG-3′ and reverse 5′-CCCCAAAGTGCCTAAGAGTG-3′; *LMO4*: forward 5′-GCAAGGCAATGTGTATCATCT-3′ and reverse 5′-GCATTCTGCAT-TACTCTGACC-3′; *Ldb1*: forward 5′-CCAGGGAGCAGAAGACAGAA-3′ and reverse 5′-AGAGGCCCAGGTTCCAAG-3′; *Ldb2*: forward 5′-TAGCC-CAAGTGCTGAAACAA-3′ and reverse 5′-TAAACTGCCCACAAAACCAA-3′; *TAL1*: forward 5′-GTTCTTAGGCTGCTGGGATG-3′ and reverse 5′-GATTTGG-GACTGAGGGAAGA-3′; *HEN1*: forward 5′-AGAGACTGAGTCGGGCTTCA-3′ and reverse 5′-CAGGCGCAGAATCTCAATCT-3′; *HEN2*: forward 5′-CCCCAAGGGTTGTGGTTTTA-3′ and reverse 5′-TCTGAACTTCTGCCCT-CATTCTTT-3′; and *GAPDH*: forward 5′-ACCTGACCTGCCGTCTAGAA-3′ and reverse 5′-TCCACCACCCTGTTGCTGTA-3′. Amplified products were electrophoretically separated on agarose gels and visualized by ethidium bromide staining. The gels were photographed under UV illumination.

Northern analysis. A human MTN blot (Clontech, Palo Alto, CA), a nylon membrane on which poly(A)$^+$ RNAs extracted from various human normal tissues were blotted, was used for analysis of the distribution of *LMO3* expression in human normal tissues. ^{32}P-labeled probe was prepared by random priming of the 2.5-kb restriction fragment of *LMO3* cDNA. The membrane was hybridized overnight at 65C in a solution containing 7.5% dextran sulfate, 1 mol/L NaCl, 1% *N*-lauroyl sarcosine, 100 μg/mL heat-denatured salmon sperm DNA, and the radiolabeled probe. The membrane was washed twice in 0.5 × SSC/0.1% *N*-lauroyl sarcosine at 50°C. Specific signals were obtained by autoradiography.

Section *in situ* hybridization. Section *in situ* hybridization was done as described previously (29). A riboprobe was synthesized with digoxygenin-UTP and T3 or T7 polymerase (Roche Molecular Biochemicals). The alkaline phosphatase reaction was done with nitroblue tetrazolium/5-bromo-4-chloro-3-indolyl phosphate (Roche Molecular Biochemicals). The riboprobe used for the section *in situ* hybridization were transcripts of the human cDNA fragments of the *LMO3* gene.

Immunohistochemistry. Neuroblastoma tissues were stained with immunoperoxidase method using anti-HEN2 antibody. They included unfavorable neuroblastomas with *MYCN* gene amplification and favorable neuroblastomas with a single copy of *MYCN* gene. Neuroblastoma specimens were fixed in 10% buffered formalin and embedded in paraffin, and 3 μm sections were applied to the immunostaining. Before incubation with anti-HEN2 antibody, the sections were treated with 0.05% Pronase in 0.05 mol/L Tris-HCl (pH 7.6) for 5 minutes. The sections were incubated with anti-HEN2 antibody, which was diluted to 1:200 at 4°C overnight. The biotin-streptavidin method (Nichirei, Tokyo, Japan) was done, and the sections were visualized with diaminobenzidine solution. The nuclei were counterstained with hematoxylin.

Immunofluorescent staining. COS7 cells were doubly transfected with the expression plasmids for HA-LMO3-A and FLAG-HEN2. Forty-eight hours after transfection, cells were fixed for 30 minutes with 3.7% formaldehyde in PBS and permeabilized with 0.2% Triton X-100 for 5 minutes, and nonspecific epitopes were blocked for 1 hour in PBS containing 3% bovine serum albumin. The cells were then incubated with a polyclonal anti-HA antibody (1:200 dilution, Medical and Biological Laboratories, Nagoya,

Japan) and a monoclonal anti-FLAG antibody (1:50, M2, Sigma Chemical). After three washes with PBS, cells were stained with a FITC- or a rhodamine-conjugated secondary antibody (1:200, Invitrogen). The coverslips were mounted onto glass slides, and the stained cells were viewed using a confocal laser scanning microscope (Olympus, Tokyo, Japan).

Western blot analysis and immunoprecipitation. After transfection, cells were rinsed twice with ice-cold PBS and then lysed immediately with SDS sample buffer. Equal amounts of proteins were separated under denaturing conditions by electrophoresis in 15% polyacrylamide gel containing SDS-PAGE and electrotransferred to polyvinylidene difluoride membrane (Immobilon-P, Millipore, Bedford, MA). After blocking in a solution containing 5% skim milk, the membrane was incubated with a monoclonal anti-FLAG, a polyclonal anti-HA, a polyclonal anti-LMO3, or a polyclonal anti-actin antibody (20-33, Sigma Chemical) and then incubated with a horseradish peroxidase–conjugated goat anti-mouse or anti-rabbit secondary antibody (Jackson ImmunoResearch Laboratories, West Grove, PA). Protein bands were visualized with an enhanced chemiluminescence (Amersham Pharmacia Biotech, Piscataway, NJ). For immunoprecipitation, transfected cells were lysed in EBC buffer [50 mmol/L Tris-HCl (pH 7.5), 120 mmol/L NaCl, 0.5% NP40, 1 mmol/L phenylmethylsulfonyl fluoride] containing protease inhibitor mixture (Sigma Chemical). The precleared soluble supernatants were mixed with a polyclonal anti-HA or a monoclonal anti-FLAG antibody and incubated for 2 hours at 4°C. Protein A-Sepharose beads were then added to the reaction mixtures and incubated for 1 hour at 4°C. The immune complexes were washed with the lysis buffer thrice at 4°C. The bound proteins were resuspended in SDS sample buffer, resolved by SDS-PAGE, and analyzed by Western blotting.

Cell proliferation and soft agar assay. Cells were seeded in triplicate in 24-well plates (5×10^3 per well) in culture medium containing 10% or 1% FBS. Cells were allowed to adhere to the bottom of the cell culture dish for 24 hours. At the indicated times, cells were trypsinized and cell counting was carried out using a Coulter Counter (Coulter Electronics Ltd., Hialeah, Finland). For soft agar assay, 2.5×10^3 cells of the stable transfectants or the parental SH-SY5Y cells were seeded in triplicate in 35-mm cell culture plates containing 0.2% agar and RPMI 1640 supplemented with 10% FBS. After 21 days, colonies with diameters >300 μm were scored as positive.

Tumor formation in nude mice. For tumor formation, 6-week-old female athymic *nu/nu* mice (Charles River Laboratory, Sulzfeld, Germany) were injected into the femur with 5×10^6 parental SH-SY5Y cells or SH-SY5Y cells transfected with the empty plasmid or with the expression plasmid encoding LMO3-A suspended in 100 μL PBS. Tumor size and body weight were measured once weekly and mice were sacrificed 7 weeks after injection. For histologic examinations, tumor tissues were fixed in fresh 10% buffered formalin and embedded in paraffin. The handling of animals was in accordance with the guidelines of the Chiba Cancer Center Research Institute (Chiba, Japan).

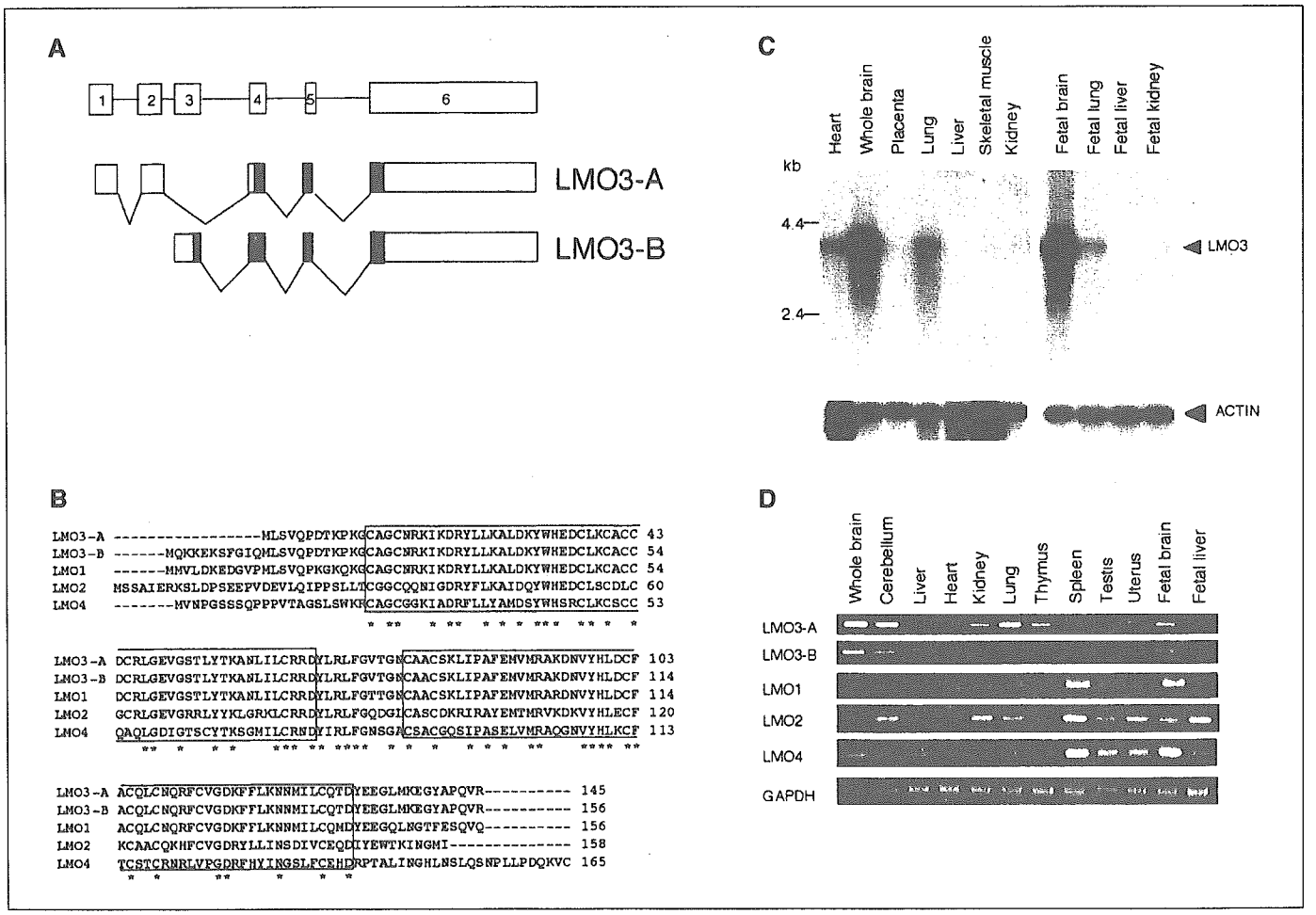

Figure 1. Identification of human LMO3-A and LMO3-B and their relation to the other LMO family members. *A*, schematic representation of the exons of human *LMO3* gene. *Solid* and *open boxes*, coding and untranslated regions, respectively. *B*, deduced amino acid sequences of human LMO3-A and LMO3-B and their alignments with those of human LMO1, LMO2, and LMO4. *Asterisks*, identical amino acid residues. Two LIM domains are *boxed*. *C*, tissue-specific expression of *LMO3*. Human multiple tissue Northern blots containing poly(A)$^+$ RNA were hybridized with a radiolabeled human *LMO3* cDNA (*top*) or with a radioactive probe derived from human *β-actin* cDNA (*bottom*). β-actin was used as a control for equal loading. The 2-kb band was hybridized ubiquitously, and an additional 1.8-kb band was hybridized in heart and skeletal muscle with the β-actin probe. *D*, coordinated expression of *LMO3-A* and *LMO3-B* in various human tissues. Total RNA isolated from the indicated human tissues was subjected to RT-PCR analysis to examine the expression levels of *LMO3-A*, *LMO3-B*, *LMO1*, *LMO2*, and *LMO4*. *GAPDH* expression is shown as an internal control.

Quantitative real-time PCR. Total RNA prepared from primary neuroblastomas was reverse transcribed into cDNA (SuperScript II kit) and subjected to the real-time PCR. The expression level of *GAPDH* was measured in all samples to normalize *LMO3* and *HEN2* expression according to the manufacturer's instructions (Applied Biosystems, Foster City, CA). Oligonucleotide primers and TaqMan probes, which were labeled at the 5′ end with the reporter dye 6-carboxyfluorescein (FAM) and at the 3′ end with the quencher dye 6-carboxytetramethylrhodamine (TAMRA), were as follows: *LMO3*: forward 5′-TCTGAGGCTCTT-TGGTGTAACG-3′, reverse 5′-CCAGGTGGTAAACATTGTCCTTG-3′, and probe 5′-FAM-AAACTGCGCTGCCTGTAGTAAGCTCATCC-TAMRA-3′ and *HEN2*: forward 5′-CCCCAAGGGTTGTGGTTTTA-3′, reverse 5′-TCTGAACTTCTGCCCTCATTCTTT-3′, and probe 5′-FAM-TTGAGTTCTCC-TACATTCATCCGCCACAA-TAMRA-3′. Amplification and detection were done using the ABI Prism 7700 Sequence Detection System (Applied Biosystems).

Statistical analysis. Student's *t* tests were used to explore possible associations between *LMO3* expression and other factors. Because the values of the *LMO3* expression were skewed, a log transformation was used to achieve the normality in the analyses using *t* test and Cox regression. The distinction between high and low levels of *LMO3* expression was based on the median value (low, *LMO3* < 0.2493 e.u.; high, *LMO3* > 0.2493 e.u.) regardless of tumor stage, *MYCN* copy number, or survival. The distinction between high and low levels of *HEN2* expression was based on the distribution of the values (low, undetectable; high, detectable). χ^2 tests were used to examine possible associations between *HEN2* expression and other factors, such as tumor stage. Kaplan-Meier survival curves were calculated, and survival distributions were compared using the log-rank test. Cox regression models were used to explore associations among *LMO3* expression, *HEN2* expression, age, *MYCN* amplification, mass screening, origin, and survival. Statistical significance was declared if $P < 0.05$. The statistical analysis was done using Stata Statistical Software Release 7.0 (Stata Corp., College Station, TX, 2001).

Results

Identification of the human *LMO3* gene. To identify the genes specifically involved in the genesis and progression of neuroblastoma, we have previously constructed cDNA libraries from the primary neuroblastomas and screened for the differentially expressed genes between the tumors with good and poor clinical outcome (25). One of the cDNA clones, *Nbla3267*, significantly overexpressed in the poor prognostic neuroblastomas contained a partial nucleotide sequence encoding a LMO family protein, LMO3. To obtain the missing 5′ part of the *LMO3* cDNA, we screened a cDNA library derived from human fetal brain. From ~6 × 10^5 recombinant phage clones, 10 independent phage clones were isolated. Sequence analysis

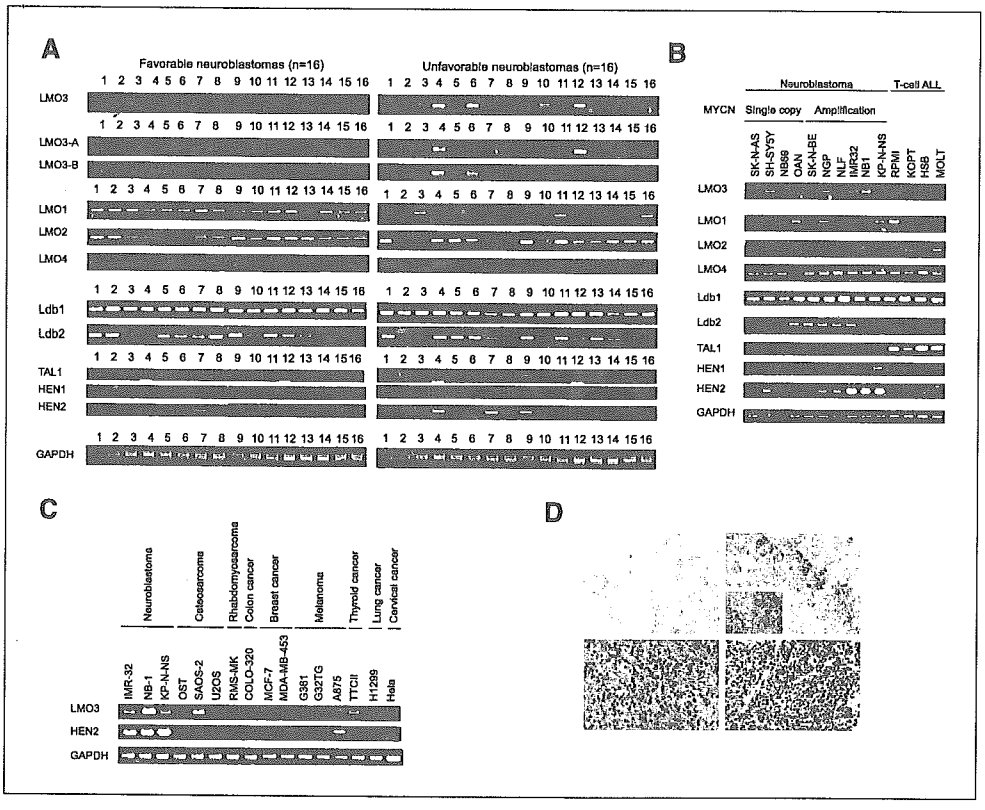

Figure 2. Increased expression of *LMO3* and *HEN2* in unfavorable neuroblastomas and neuroblastoma-derived cell lines. *A*, expression of *LMO3* and *LMO*-related genes in primary neuroblastomas with favorable (stage I, a single copy of *MYCN* and high expression of *TrkA*) and unfavorable (stages III and IV, *MYCN* amplification and decreased expression of *TrkA*) characteristics. Total RNA was isolated from the indicated neuroblastoma tissues, reverse transcribed, and amplified by PCR to examine the expression levels of *LMO3*, *LMO3-A*, *LMO3-B*, *LMO1*, *LMO2*, *LMO4*, *Ldb1*, *Ldb2*, *TAL1*, *HEN1*, and *HEN2*. Expression of *GAPDH* serves as an internal control. PCR products were visualized by ethidium bromide staining. *B*, expression of *LMO3* and *LMO*-related genes in neuroblastoma cell lines without *MYCN* amplification (SK-N-AS, SH-SY5Y, NB69, and OAN), neuroblastoma cell lines with *MYCN* amplification (SK-N-BE, NGP, NLF, IMR32, NB1, and KP-N-NS), and ALL cell lines (RPMI, KOPT, HSB, and MOLT). Total RNA prepared from the indicated cultured cells was subjected to RT-PCR analysis. Expression of *GAPDH* serves as an internal control. *C*, expression of *LMO3* and *HEN2* in various tumor-derived cell lines. Total RNA prepared from the indicated culture cells was subjected to RT-PCR analysis as described above. *D*, section *in situ* hybridization of neuroblastoma with the *LMO3* probe. Serial sections of the favorable neuroblastoma tissue (*top left* and *inset*) or the unfavorable one with *MYCN* amplification (*top right* and *inset*) were prepared, and expression of the *LMO3* gene was examined by section *in situ* hybridization. The *LMO3* transcripts are positive in unfavorable neuroblastoma. Immunohistochemical staining of HEN2 in primary neuroblastoma tissues. HEN2 is strongly positive in the nucleus of most tumor cells with *MYCN* amplification (*bottom right*), whereas it is negative in the favorable neuroblastoma tissue (*bottom left*).

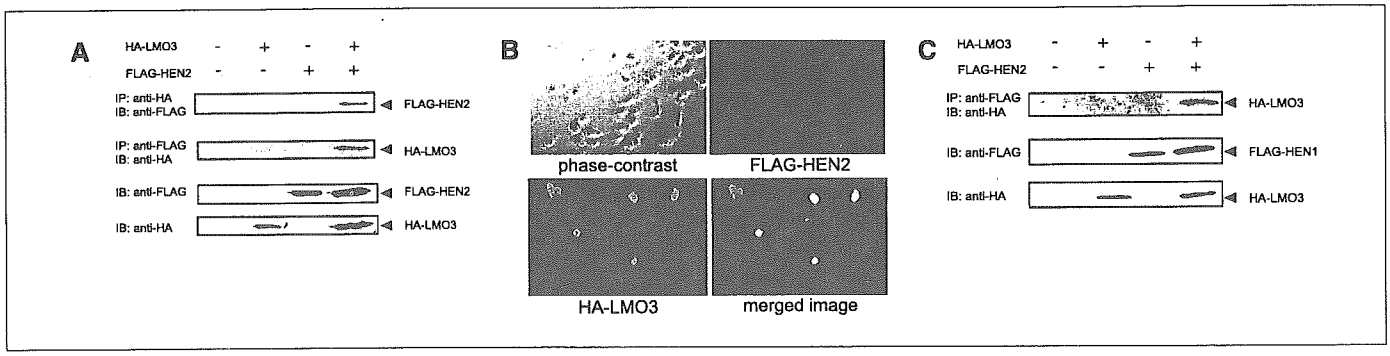

Figure 3. LMO3 interacts with HEN2 in mammalian cells. *A,* coimmunoprecipitation analysis. COS7 cells were transfected with the indicated expression plasmids. Forty-eight hours after transfection, whole cell lysates were prepared and subjected to the immunoprecipitation/Western analysis (*top* and *top middle*). Whole cell lysates were monitored on immunoblot for the expression of FLAG-HEN2 (*bottom middle*) and HA-LMO3-A (*bottom*). *B,* nuclear colocalization of LMO3 and HEN2 in cultured cells. COS7 cells were cotransfected with the expression plasmids for HA-LMO3-A and FLAG-HEN2. Forty-eight hours after transfection, cells were fixed and incubated with the polyclonal anti-HA and monoclonal anti-FLAG antibodies. Cells were then processed for double immunofluorescence using the FITC-conjugated anti-rabbit IgG (*green*) and with the rhodamine-conjugated anti-mouse IgG (*red*). The merged images (*yellow*) suggest the nuclear colocalization of LMO3 and HEN2. The phase-contrast images are also shown. *C,* coimmunoprecipitation of FLAG-HEN1 and HA-LMO3. Whole cell lysates prepared from COS7 cells transfected with the indicated combinations of the expression plasmids were immunoprecipitated with the anti-FLAG antibody followed by immunoblotting with the anti-HA antibody (*top*). Levels of FLAG-HEN1 and HA-LMO3 were also examined by immunoblotting with the anti-FLAG antibody (*middle*) and with the anti-HA antibody (*bottom*), respectively.

revealed that they were divided into two types, designated LMO3-A (145 amino acids) and LMO3-B (156 amino acids), with the different translation initiation sites. The NH_2-terminal region of LMO3-A was identical to that of the previously reported LMO3 protein (11). As shown in Fig. 1*A*, the putative translation initiation sites of LMO3-A and LMO3-B were located within exons 4 and 3, respectively. Because *LMO3* is a single gene, it is likely that LMO3-A and LMO3-B arise from differential splicing

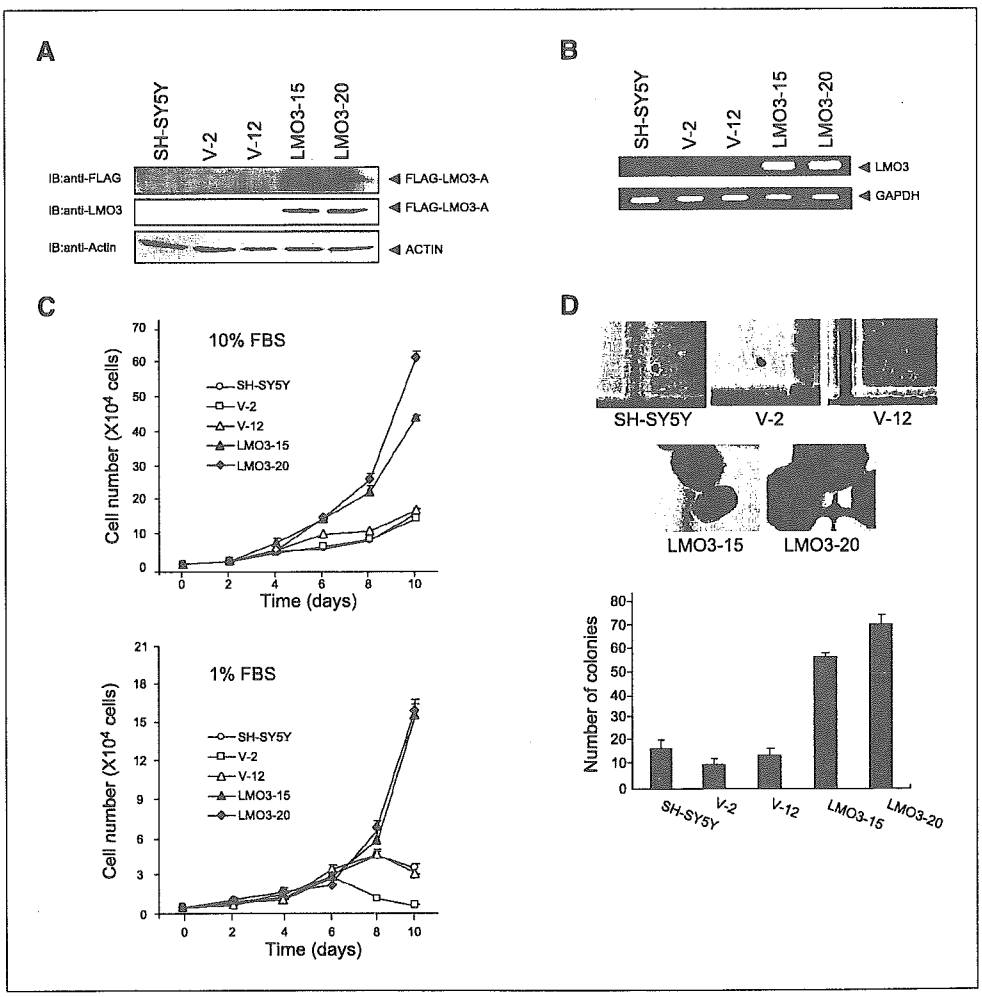

Figure 4. Growth-promoting activity of LMO3 in SH-SY5Y cells. *A,* stable SH-SY5Y transfectants expressing exogenous FLAG-LMO3-A. SH-SY5Y cells were stably transfected with the empty plasmid or with the expression plasmid for FLAG-LMO3-A and maintained in the presence of G418 (at a final concentration of 400 μg/mL) for 3 weeks. Whole cell lysates prepared from the indicated drug-resistant cell clones in addition to the parental SH-SY5Y cells were subjected to Western blot analysis using the anti-FLAG (*top*), anti-LMO3 (*middle*), or anti-actin (*bottom*) antibody. *B,* RT-PCR analysis of LMO3 in the indicated stable transfectants along with the parental SH-SY5Y cells. Expression of GAPDH serves as an internal control. *C,* effects of LMO3 overexpression on cell growth in SH-SY5Y cells. SH-SY5Y cells and the indicated transfectants were grown in the culture medium containing 10% (*top*) or 1% (*bottom*) FBS. Cells were harvested at 48-hour time intervals and number of cells was counted in triplicate. *Points,* means from three independent experiments; *bars,* SE. *D,* anchorage-independent growth of LMO3-overexpressing transfectants. The parental SH-SY5Y cells and the indicated transfectants (2.5×10^3 cells per dish) were grown in soft agar medium. After 3 weeks of culture, cells were examined by phase-contrast microscopy (*top*), and the numbers of colonies with a diameter of >300 μm were counted (*bottom*). *Columns,* means from three independent experiments; *bars,* SE.

or alternative promoter usage. Amino acid sequence alignment of LMO3 with the other LMO family proteins (LMO1, LMO2, and LMO4) showed a significant homology among them (Fig. 1*B*). LIM domains of LMO3 presented 98%, 60%, and 55% amino acid homology with those of LMO1, LMO2, and LMO4, respectively.

To determine the expression pattern of human *LMO3* mRNA, we did Northern blot analysis on a human multiple tissues blot using -actin as a control. As shown in Fig. 1*C*, *LMO3* mRNA (~4 kb) was abundantly expressed in brain and at relatively low levels in the heart and lung but not in the other tissues examined. Similar to the adult tissues, *LMO3* mRNA was expressed predominantly in fetal brain, with a lower level in fetal lung. We then compared the tissue distribution of *LMO3-A* expression with those of *LMO3-B* and the other *LMO* family gene expression in various human adult and fetal tissues by RT-PCR (Fig. 1*D*). The expression pattern of *LMO3-A* was similar to that of *LMO3-B*, with relatively higher levels in brain, cerebellum, and fetal brain. In contrast, *LMO2* and *LMO4* were expressed ubiquitously in human tissues, and *LMO1* was expressed at higher levels in spleen and fetal brain.

Expression of *LMO3* and *HEN2* in aggressive neuroblastomas. As described previously, LMO family protein interacts with the nuclear LIM domain–binding protein 1 and 2 (Ldb1 and Ldb2), which act as adaptors for several LIM domain–containing proteins (30–32), and also binds to the basic helix-loop-helix transcription factor, TAL1, to regulate its transcriptional activity (12, 33, 34). Of interest, HEN1 and HEN2 were previously identified based on their homology with TAL1, and it was shown that LMO3 was associated with HEN1 (35). Furthermore, TAL1 was coexpressed with LMO1 or LMO2 in T-cell ALL (36), and double transgenic mice overexpressing TAL1 and LMO1 or LMO2 developed leukemia (37). As shown in Fig. 2*A*, *LMO3* (A and B) and *HEN2* were expressed at higher levels in unfavorable neuroblastomas compared with favorable tumors, whereas the levels of *LMO1* expression were predominantly high in the favorable tumors. No significant changes in the expression levels of *LMO2*, *Ldb1*, and *Ldb2* were detected between unfavorable and favorable neuroblastomas. *LMO4*, *TAL1*, and *HEN1* showed extremely low levels of expression in both types of neuroblastoma. We then studied the expression of these genes in 10 neuroblastoma and 4 T-cell ALL cell lines to examine the presence or absence of the lineage specificity, neuronal or hematopoietic. Consistent with the previous reports (36), *LMO2* and *TAL1* were coexpressed in T-cell ALL-derived cell lines (RPMI, KOPT, HSB, and MOLT; Fig. 2*B*). However, of interest, *LMO3* and *Ldb2* were expressed predominantly in neuroblastoma cell lines compared with the leukemia-derived lines. In addition, *HEN2* tended to be less highly expressed in leukemia cells compared with neuroblastoma cells. *HEN1* expression was also restricted to neuroblastoma but limited to only a few cell lines. On the other hand, there was no difference in the expression of *LMO4* and *Ldb1* between neuroblastoma-derived and T-cell ALL-derived cell lines. Interestingly, coexpression of *LMO3* and *HEN2* was observed in the majority of neuroblastoma cell lines but not in the other tumor-derived cell lines with different origin (Fig. 2*C*). These results revealed that only *LMO3* and *HEN2* were expressed at high levels in aggressive neuroblastomas in a neuronal-specific pattern.

Figure 2*D* shows the results of *in situ* hybridization for *LMO3* in primary neuroblastomas. *LMO3* mRNA was expressed in a stage IV neuroblastoma with *MYCN* amplification, whereas it was negative in a stage I tumor with a single copy of *MYCN* and high expression of *TrkA*. Unfortunately, our antibody raised against human LMO3 protein did not work for the immunohistochemical analysis. The immunostaining of HEN2 was also strongly positive in the nuclei of most tumor cells in *MYCN*-amplified neuroblastoma, albeit it was negative in favorable subset of the tumor (Fig. 2*D*).

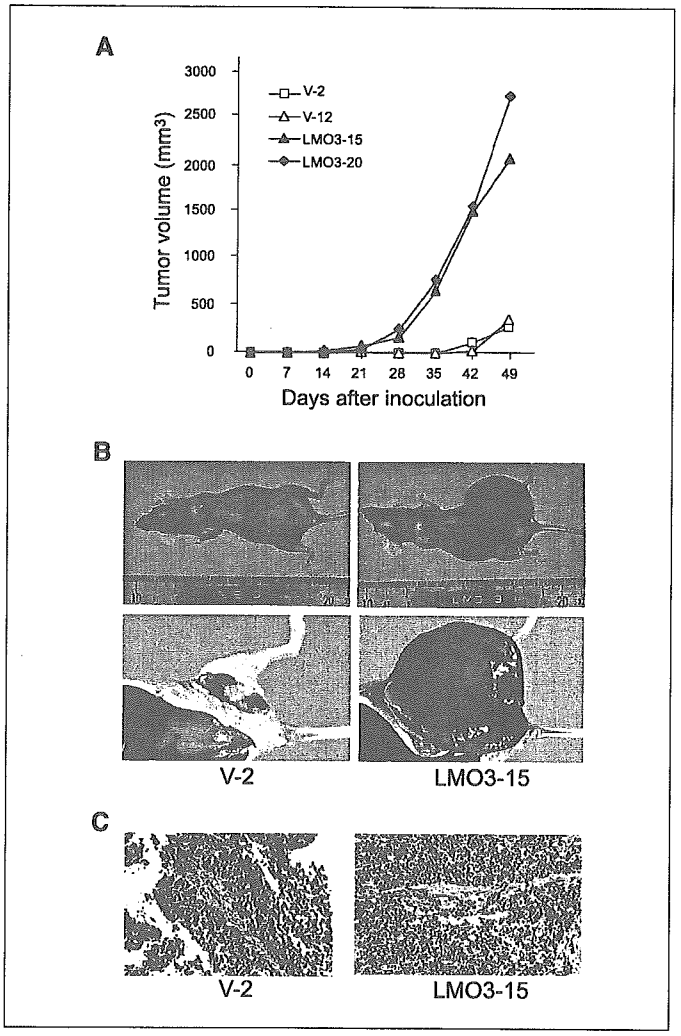

Figure 5. Tumor growth in nude mice. *A*, nude mice were injected s.c. with 5×10^6 of SH-SY5Y cells or the indicated stable transfectants and tumor volumes were estimated weekly. *Points*, mean of 8 to 11 independent tumors. *B*, photographs of the tumors 49 days after s.c. injection of V-2 (*left*) and LMO3-15 cells (*right*) into nude mice. *C*, paraffin sections of the tumors arising from V-2 (*left*) and LMO3-15 cells (*right*) were stained with H&E.

LMO3 physically interacts with HEN2. Because LMO3 and HEN2 were coexpressed in the majority of unfavorable neuroblastomas as well as neuroblastoma cell lines, we examined whether LMO3 could interact with HEN2 in mammalian cells. Whole cell lysates prepared from COS7 cells transfected with the expression plasmids for HA-tagged LMO3 and FLAG-tagged HEN2 were immunoprecipitated with the anti-HA or with the anti-FLAG antibody followed by immunoblotting with the anti-FLAG or with the anti-HA antibody, respectively. As shown in Fig. 3*A*, FLAG-HEN2 was coimmunoprecipitated with HA-LMO3. We then examined the subcellular distribution of LMO3 and